

Electronic supporting information

for

Noncovalent binding of tripeptides containing tryptophan to polynucleotides and photochemical deamination of modified tyrosine to quinone methide leading to covalent attachment

Antonija Erben,^a Igor Sviben,^a Branka Mihaljević,^b Ivo Piantanida,^a Nikola Basarić^{a*}

^a Department of Organic Chemistry and Biochemistry, Ruđer Bošković Institute, Bijenička cesta 54, 10 000 Zagreb, Croatia. Fax: + 385 1 4680 195; Tel: +385 1 4680 196

^b Department of Material Chemistry, Ruđer Bošković Institute, Bijenička cesta 54, 10 000 Zagreb

Corresponding author's E-mail address: nbasarić@irb.hr

Content:

1. Synthetic procedure for the preparation of known compounds (Eqs S1-S5, Tables S1 and S2)	S2
2. UV-vis and fluorescence data (Figs S1-S10, Eq S6 and S7)	S9
3. Laser flash photolysis (Figs S11-S35)	S14
4. Non-covalent binding to polynucleotides (Figs S38-S54, Table S3, Eq S8)	S25
5. Covalent binding to oligonucleotides (Fig S55-S75 and Table S4)	S35
6. NMR spectra	S46
7. References	S61

1. Synthetic procedure for the preparation of known compounds

***N*-Boc-L-Tyr[CH₂N(CH₃)₂]-OBn¹**

A flask was charged with *N*-Boc-L-Tyr-OBn (1.11 g, 3.0 mmol) dissolved in CH₂Cl₂ (150 mL). To the reaction mixture, K₂CO₃ (0.21 g, 1.5 mmol) and Eschenmoser's salt (0.28 g, 3.0 mmol) were added and the reaction was stirred at rt for 5 days. When the reaction was finished, the reaction mixture was filtered through a sinter funnel, and from the filtrate the solvent was removed on a rotary evaporator. The product was purified by column chromatography on aluminum oxide (III) using 0→5% CH₃OH in CH₂Cl₂ to afford the pure product (0.72 g, 56 %) in the form of colorless crystals.

¹H NMR (CD₃OD, 300 MHz) δ/ppm: 7.35-7.22 (m, 5H), 6.91 (dd, *J*= 1.6, 8.0 Hz, 1H), 6.84 (d, *J*= 1.6 Hz, 1H), 6.64 (d, *J*= 8.0 Hz, 1H), 5.12 (d, *J*= 12.0 Hz, 1H), 5.06 (d, *J*= 12.0 Hz, 1H), 4.37-4.23 (m, 1H), 3.53 (s, 2H), 2.96 (dd, *J*= 6.4, 13.6 Hz, 1H), 2.84 (dd, *J*= 13.6, 8.0 Hz, 1H), 2.26 (s, 6H), 1.38 (s, 9H); ¹³C NMR (CD₃OD, 75 MHz) δ/ppm: 173.7 (s, 1C), 157.8 (s, 1C), 157.7 (s, 1C), 137.1 (s, 1C), 131.1 (d, 2C), 130.5 (d, 3C), 129.5 (d, 1C), 129.3 (d, 1C), 128.6 (s, 1C), 123.5 (s, 1C), 116.6 (d, 1C), 80.6 (s, 1C), 67.8 (t, 1C), 62.4 (t, 1C), 56.9 (d, 1C), 44.7 (q, 2C), 37.9 (t, 1C), 28.6 (q, 3C).

TFA×H-L-Tyr[CH₂N(CH₃)₂×TFA]-OBn¹

N-Boc-L-Tyr[CH₂N(CH₃)₂]-OBn (335 mg, 0.8 mmol) was dissolved in CH₂Cl₂ (3 mL). TFA/CH₂Cl₂ (1:1, 4 mL) was added and the reaction mixture was stirred at rt 2 h. The solvent was removed by distillation in vacuum to afford oily product quantitatively.

¹H NMR (CD₃OD, 300 MHz) δ/ppm: 7.41-7.28 (m, 5H), 7.14-7.09 (m, 2H), 6.86 (d, *J*= 8.8 Hz, 1H), 5.26 (d, *J*= 11.5 Hz, 1H), 5.20 (d, *J*= 11.5 Hz, 1H), 4.31 (dd (t), *J*= 7.0 Hz), 4.22 (d, *J*= 12.9 Hz, 1H), 4.13 (d, *J*= 12.9 Hz, 1H), 3.15 (d, *J*= 7.5 Hz, 2H), 2.79 (d, *J*= 7.5 Hz, 6H); ¹³C NMR (CD₃OD, 75 MHz) δ/ppm: 169.9 (s, 1C), 157.5 (s, 1C), 136.2 (s, 1C), 134.4 (d, 1C), 134.0 (d, 1C), 129.9 (d, 1C), 129.8 (d, 2C), 129.7 (d, 2C), 126.6 (s, 1C), 118.0 (s, 1C), 117.0 (d, 1C), 69.3 (t, 1C), 58.2 (t, 1C), 55.2 (d, 1C), 43.2 (q, 2C), 36.5 (t, 1C).

***N*-Boc-L-Trp-OSu²**

N-Boc-L-Trp (5.00 g, 16.4 mmol), *N*-hydroxysuccinimide (NHS, 2.07 g, 18.0 mmol) and *N,N'*-dicyclohexylcarbodiimide (DCC, 3.72 g, 18.0 mmol) were dissolved in CH₂Cl₂ (40 mL). The reaction mixture was stirred for 2 h and cooled by an ice bath, and after that kept in a refrigerator overnight. The precipitate was filtered off and the solvent was removed on a rotary evaporator.

The residue was suspended in EtOAc (100 mL) and left to stand in a refrigerator. After filtration, the solution was washed with aqueous Na₂CO₃ (0.5 M, 100 mL), HCl (0.5 M, 100 mL) and water (100 mL). The organic solution was dried over anhydrous MgSO₄, filtered and the solvent was removed on a rotary evaporator to afford yellowish product (6.07 g, 89%), which was used in the next step without purification.

¹H NMR (CD₃OD, 300 MHz) δ /ppm: 7.58 (d, J = 7.5 Hz, 1H), 7.33 (d, J = 8.0 Hz, 1H), 7.22 (br. s, 1H), 7.10 (dd (t), J = 8.0 Hz, 1H), 7.03 (dd (t), J = 8.0 Hz, 1H), 4.80 (dd, J = 5.0, 8.0 Hz, 1H), 3.47 (dd, J = 5.0, 14.7 Hz, 1H), 3.22 (dd, J = 8.0, 14.7 Hz, 1H), 2.84 (s, 4H), 1.36 (s, 9H).

***N*-Boc-L-Trp- L-Trp-OH³**

A solution of *N*-Boc-L-Trp-OSu (2.21 g, 5.5 mmol) in THF (25 mL) was added slowly to the suspension of L-Trp (1.02 g, 5.0 mmol) and NaHCO₃ (0.84 g, 10.0 mmol) in a mixture of THF and H₂O (1:1, 48 mL). The reaction mixture was stirred at rt for 3 days. THF was removed on a rotary evaporator and the aqueous residue acidified with HCl (0.5 M) to pH 2-3. An extraction with EtOAc (3×50 mL) was carried out, the extracts were dried over anhydrous Na₂SO₄, filtered and the solvent was removed on a rotary evaporator to afford product in the form of colorless solid (2.34 g, 95%).

¹H NMR (CD₃OD, 300 MHz) δ /ppm: 7.57 (d, J = 7.9 Hz, 1H), 7.32 (dd (t), J = 7.9 Hz, 3H), 7.13-6.96 (m, 5H), 6.90 (dd (t), J = 6.5 Hz 1H), 4.77-4.67 (m, 1H), 4.37-4.27 (m, 1H), 3.25-3.13 (m, 3H), 3.09-2.97 (m, 1H), 1.28 (s, 9H); ¹³C NMR (CD₃OD, 75 MHz) δ /ppm: 174.9 (s, 1C), 174.4 (s, 1C), 157.4 (s, 1C), 138.1 (s, 1C), 137.9 (s, 1C), 128.9 (s, 1C), 128.8 (s, 1C), 124.7 (d, 1C), 124.5 (d, 1C), 122.42 (d, 1C), 122.40 (d, 1C), 119.85 (d, 1C), 119.81 (d, 1C), 119.4 (d, 1C), 119.2 (d, 1C), 112.3 (d, 1C), 112.2 (d, 1C), 110.9 (s, 1C), 110.4 (s, 1C), 80.7 (s, 1C), 56.7 (d, 1C), 54.6 (d, 1C), 28.9 (t, 1C), 28.5 (q, 3C), 28.3 (t, 1C).

***N*-Boc-L-Trp-L-Trp-OSu²**

N-Boc-L-Trp-L-Trp (0.96 g, 2.0 mmol), NHS (0.25 g, 2.2 mmol) and DCC (0.34 g, 2.2 mmol) were dissolved in CH₂Cl₂ (15 mL). The reaction mixture was stirred for 2 h and cooled by an ice bath, and after that kept in a refrigerator overnight. The reaction mixture was washed with aqueous Na₂CO₃ (0.5 M, 75 mL), HCl (0.5 M, 75 mL) and water (75 mL). The organic solution was dried over anhydrous Na₂SO₄, filtered and the solvent was removed on a rotary evaporator to afford product in the form of colorless solid (0.70 g, 60%), which was used in the next step without purification.

^1H NMR (CD_3OD , 300 MHz) δ/ppm : 7.55 (d, $J = 7.7$ Hz, 1H), 7.37-7.26 (m, 2H), 7.20 (br. s, 1H), 7.14-6.80 (m, 6H), 5.13 (dd (t), $J = 6.1$ Hz, 1H), 4.37-4.25 (m, 1H), 3.35-3.00 (m, 4H), 2.81 (s, 4H), 1.25 (s, 9H).

Synthesis of tripeptides – general procedure

A solution of *N*-Boc-L-Trp-L-Trp-OSu (387 mg, 0.65 mmol) in THF-u (6 mL) was added slowly to a suspension of the salt $\text{TFA} \times \text{H-L-Tyr-OBn}$ or $\text{TFA} \times \text{H-L-Phe-OBn}$ (0.6 mmol) and NaHCO_3 (252 mg, 3.0 mmol) in a mixture of THF and H_2O (1:1, 12 mL). The reaction mixture was stirred at rt over 3 days. THF was removed on a rotary evaporator and the aqueous residue was acidified by HCl (0.5 M) to the pH value of 2-3. The extraction with EtOAc (3×50 mL) was carried out and the extracts were dried over anhydrous sodium sulfate. After filtration, the solvent was removed on a rotary evaporator and the crude residue was purified on a column of silica gel using $\text{CH}_3\text{OH}/\text{CH}_2\text{Cl}_2$ (1 \rightarrow 20%) as eluent to afford the pure oily product.

N-Boc-L-Trp- L-Trp-L-Phe-OBn (1)³

Prepared according to the general procedure from *N*-Boc-L-Trp-L-Trp-OH (387 mg, 0.65 mmol) and $\text{TFA} \times \text{H-L-Phe-OBn}$ (0.24 g, 0.6 mmol). After column chromatography, the oily product was obtained (0.25 g, 30%).

^1H NMR (CD_3OD , 300 MHz) δ/ppm : 7.56 (d, $J = 8.0$ Hz, 1H), 7.36 (d, $J = 8.4$ Hz, 1H), 7.33-7.26 (m, 4H), 7.24-7.18 (m, 2H), 7.18-7.12 (m, 4H), 7.12-7.07 (m, 2H), 7.05-6.97 (m, 4H), 6.93-6.86 (m, 1H), 6.82 (br. s, 1H), 5.04 (d, $J = 12.0$ Hz, 1H), 4.98 (d, $J = 12.0$ Hz, 1H), 4.61-4.52 (m, 2H), 4.23 (dd (t), $J = 5.6$ Hz, 1H), 3.18-3.02 (m, 3H), 2.97-2.87 (m, 1H), 2.83-2.67 (m, 2H), 1.22 (s, 9H); ^{13}C NMR (CD_3OD , 150 MHz) δ/ppm : 174.3 (s, 1C), 173.4 (s, 1C), 172.1 (s, 1C), 138.1 (s, 1C), 138.0 (s, 1C), 137.7 (s, 1C), 137.0 (s, 1C), 130.2 (d, 2C), 129.5 (d, 4C), 129.4 (d, 2C), 129.3 (d, 1C), 128.9 (s, 1C), 128.8 (s, 1C), 127.9 (d, 1C), 124.9 (d, 1C), 124.8 (d, 1C), 122.6 (d, 1C), 122.5 (d, 1C), 120.0 (d, 2C), 119.5 (d, 1C), 119.2 (d, 1C), 112.4 (d, 2C), 110.7 (s, 1C), 110.0 (s, 1C), 80.9 (s, 1C), 67.9 (t, 1C), 57.1 (d, 1C), 55.6 (d, 1C), 55.1 (d, 1C), 38.6 (t, 1C), 28.6 (t, 1C), 28.5 (q, 3C), 28.1 (t, 1C).

N-Boc-L-Trp-L-Trp-L-Tyr-OBn (2)³

Prepared according to the general procedure from *N*-Boc-L-Trp-L-Trp-OH (387 mg, 0.65 mmol) and $\text{TFA} \times \text{H-L-Tyr-OBn}$ (0.23 g, 0.6 mmol). After column chromatography, the oily product was obtained (0.13 g, 30%).

^1H NMR (CD_3OD , 300 MHz) δ/ppm : 7.56 (d, J = 7.8 Hz, 1H), 7.39-7.24 (m, 5H), 7.24-7.16 (m, 1H), 7.16-6.96 (m, 6H), 6.96-6.76 (m, 4H), 6.62 (d, J = 8.4 Hz, 2H), 5.03 (d, J = 13.0 Hz, 1H), 4.99 (d, J = 13.0 Hz, 1H), 4.60-4.46 (m, 2H), 4.24 (dd (t), J = 6.5 Hz, 1H), 3.19-3.02 (m, 3H), 2.87-2.65 (m, 3H), 1.22 (s, 9H); ^{13}C NMR (CD_3OD , 75 MHz) δ/ppm : 174.6 (s, 1C), 173.5 (s, 1C), 172.5 (s, 1C), 157.4 (s, 1C), 138.04 (s, 1C), 138.00 (s, 1C), 137.0 (s, 1C), 131.4 (d, 2C), 129.5 (d, 2C), 129.3 (d, 1C), 129.2 (d, 1C), 128.8 (s, 1C), 128.7 (d, 1C), 128.3 (s, 1C), 124.7 (d, 1C), 124.6 (d, 1C), 122.5 (d, 2C), 120.0 (d, 1C), 119.9 (d, 1C), 119.44 (d, 1C), 119.40 (d, 1C), 116.3 (d, 1C), 112.3 (d, 2C), 110.9 (s, 1C), 110.3 (s, 1C), 80.7 (s, 1C), 67.4 (t, 1C), 57.5 (d, 1C), 55.8 (d, 1C), 55.1 (d, 1C), 37.8 (t, 1C), 29.0 (t, 1C), 28.7 (q, 3C), 28.5 (t, 1C).

Removal of Boc – general procedure

Tripeptide **1-3** (0.03 mmol) was dissolved in anhydrous EtOAc to which a saturated solution of HCl in EtOAc was added (5 M, 1 mL). The reaction mixture was stirred 1 h at rt and the solvent was removed in vacuum. The remaining crystals were washed with Et_2O and dried on a rotary evaporator. The product was purified by preparative TLC on silica gel using 20% MeOH/ CH_2Cl_2 as eluent or by semipreparative HPLC.

HCl \times H-L-Trp-L-Trp-L-Phe-OBn (1 \times HCl)³

Prepared according to the general procedure from **1** (20 mg, 0.03 mmol) giving the oily product (10 mg, 55%).

^1H NMR (CD_3OD , 300 MHz) δ/ppm : 7.64 (d, J = 8.1 Hz, 1H), 7.58 (d, J = 7.8 Hz, 1H), 7.37 (dd (t), J = 8.1 Hz, 2H), 7.33-7.27 (m, 3H), 7.26-7.21 (m, 3H), 7.20-7.15 (m, 3H), 7.14-7.05 (m, 6H), 7.04-6.96 (m, 3H), 5.08 (d, J = 12.1 Hz, 1H), 5.02 (d, J = 12.1 Hz, 1H), 4.73 (dd (t), J = 7.0 Hz, 1H), 4.65 (dd, J = 6.4, 7.8 Hz, 1H), 4.07 (dd, J = 5.6, 8.7 Hz, 1H), 3.21 (dd, J = 6.4, 14.7 Hz, 1H), 3.15-3.02 (m, 3H), 2.94 (dd, J = 7.8, 13.7 Hz, 1H); ^{13}C NMR (CD_3OD , 150 MHz) δ/ppm : 173.2 (s, 1C), 172.3 (s, 1C), 169.8 (s, 1C), 138.3 (s, 1C), 138.1 (s, 1C), 137.8 (s, 1C), 136.9 (s, 1C), 130.4 (d, 1C), 129.5 (d, 3C), 129.4 (d, 1C), 128.7 (s, 1C), 128.2 (s, 1C), 127.9 (d, 1C), 125.8 (d, 1C), 124.8 (d, 1C), 122.9 (d, 1C), 122.5 (d, 1C), 120.3 (d, 1C), 119.8 (d, 1C), 119.4 (d, 1C), 119.3 (d, 1C), 119.1 (d, 1C), 112.6 (d, 1C), 112.4 (d, 1C), 110.5 (s, 1C), 107.9 (s, 1C), 68.0 (t, 1C), 55.55 (d, 1C), 55.53 (d, 1C), 54.7 (d, 1C), 38.4 (t, 1C), 29.2 (t, 1C), 28.9 (t, 1C).

HCl \times H-L-Trp-L-Trp-L-Tyr-OBn (2 \times HCl)³

Prepared according to the general procedure from **2** (20 mg, 0.03 mmol) giving the oily product (11 mg, 61%).

¹H NMR (CD₃OD, 600 MHz) δ /ppm: 7.61 (d, *J* = 8.0 Hz, 1H), 7.44 (d, *J* = 8.0 Hz, 1H), 7.36 (d, *J* = 8.0 Hz, 1H), 7.34-7.29 (m, 4H), 7.22 (dd, *J* = 1.8, 7.0 Hz, 2H), 7.11 (dd(t), *J* = 7.5 Hz 1H), 7.09-7.05 (m, 2H), 7.02 (dd(t), *J* = 7.5 Hz 1H), 6.97-6.93 (m, 2H), 6.85 (d, *J* = 8.3 Hz, 2H), 6.65 (d, *J* = 8.3 Hz, 2H), 5.05 (d, *J* = 12.0 Hz, 1H), 5.03 (d, *J* = 12.0 Hz, 1H), 4.69 (dd(t), *J* = 6.9 Hz, 1H), 4.57 (dd(t), *J* = 7.0 Hz, 1H), 3.85 (dd(t), *J* = 6.5 Hz, 1H), 3.21 (dd, *J* = 5.5, 14.6 Hz, 1H), 3.10-3.00 (m, 4H), 2.91 (dd, *J* = 6.5, 14.0 Hz, 1H), 2.82 (dd, *J* = 7.4, 14.0 Hz, 1H); **¹³C NMR** (CD₃OD, 150 MHz) δ /ppm: 176.2 (s, 1C), 173.5 (s, 1C), 172.4 (s, 1C), 157.4 (s, 1C), 138.2 (s, 1C), 138.0 (s, 1C), 131.4 (d, 2C), 129.52 (d, 2C), 129.51 (d, 2C), 129.3 (d, 1C), 128.85 (s, 1C), 128.83 (s, 1C), 128.2 (s, 1C), 125.0 (d, 1C), 124.8 (d, 1C), 122.6 (d, 1C), 122.4 (d, 1C), 120.0 (d, 1C), 119.8 (d, 1C), 119.5 (d, 1C), 119.4 (d, 1C), 116.3 (d, 1C), 112.4 (d, 1C), 112.3 (d, 1C), 110.6 (s, 1C), 110.3 (s, 1C), 67.9 (t, 1C), 56.1 (d, 1C), 55.5 (d, 1C), 55.0 (d, 1C), 37.7 (t, 1C), 31.1 (t, 1C), 28.8 (t, 1C).

HPLC analysis and separation

Analysis of the samples was performed by HPLC on a Phenomenex Luna C18

Table S1. The following method was used:

<i>t</i> / min	B (%)
0	100
10	100
20	0
30	0

A: CH₃OH, 100 %

B: CH₃OH-H₂O (1:1 v/v) + TFA, 0.1%

Flow rate: 1 mL/ min.

Semipreparative HPLC separation on a Phenomenex Jupiter C18 5 μ 300A column

Table S2. The following method was used:

t / min	B (%)
0	100
20	100
40	0
60	0

A: CH₃OH, 100 %

B: CH₃OH-H₂O (1:1 v/v) + TFA, 0.1%

Flow rate: 1 mL/ min.

Determination of the quantum yield of photomethanolysis

The **number of absorbed photons for the KIO₃/KI** was calculated from:

$$n(\text{absorbed photons}) = \frac{\Delta A_{352} \times V_{\text{irr}}}{\epsilon_{352} \times \ell \times \Phi_{\text{lit.}}} \quad (\text{S1})$$

where:

ΔA_{352} absorbance difference at 352 nm for the irradiated and non-irradiated sample

V_{irr} volume of the solution which was irradiated

ϵ_{352} molar absorption coefficient for I₃⁻ in solution which contains iodides and iodates, 27600 M⁻¹ cm⁻¹

ℓ length of the optical path (1 cm in all experiments)

$\Phi_{\text{lit.}}$ quantum yield ($\Phi_{254} \approx 0.74$), the precise value was calculated from S2 and S3 (depending on the iodine concentration and temperature)

$$c(\text{I}^-) = A_{300} / 1.061 \quad [\text{M}] \quad (\text{S2})$$

$$\Phi_{\text{lit}} = 0.75 \times [1 + 0.02(T - 20.7)] \times [1 + 0.23(c(\text{I}^-) - 0.577)] \quad (\text{S3})$$

For the absorbances in the range 0.4-0.8 the number of absorbed photons was calculated according to:

$$n(\text{absorbed photons}) = n(\text{total photons}) \times (1-T) \quad (\text{S4})$$

The quantum yield for the photohydrolysis was calculated according to:

$$\Phi = \frac{A_{254} \cdot V_{\text{irr}} \cdot x(\text{photoproduct})_{\text{HPLC}}}{\epsilon_{254} \cdot \ell \cdot n(\text{total photons}) \cdot (1 - T_{254})} \quad (\text{S5})$$

where:

$x(\text{photoproduct})_{\text{HPLC}}$ conversion of reactant to photoproduct determined by HPLC

T_{254} transmittance of light at 254 nm

2. UV-vis and fluorescence data

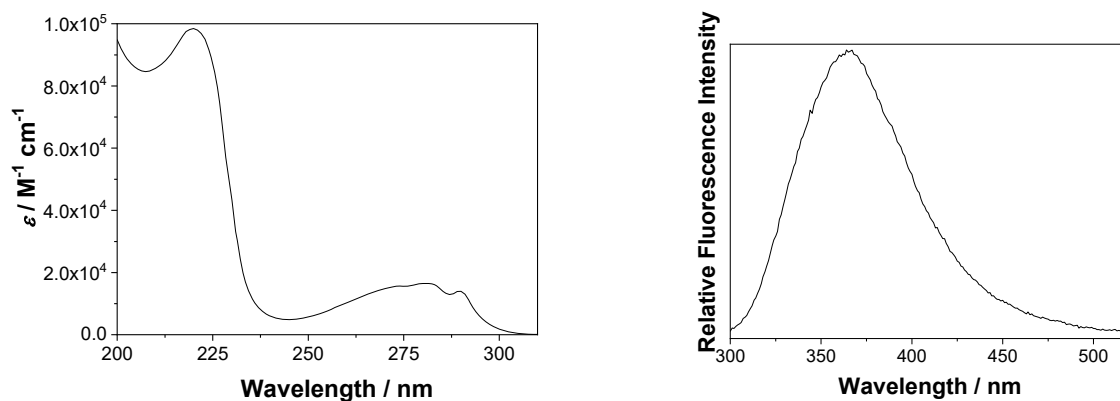


Fig. S1. Absorption spectrum (left) and emission spectrum ($\lambda_{\text{ex}} = 280 \text{ nm}$) of **1** in CH_3CN .

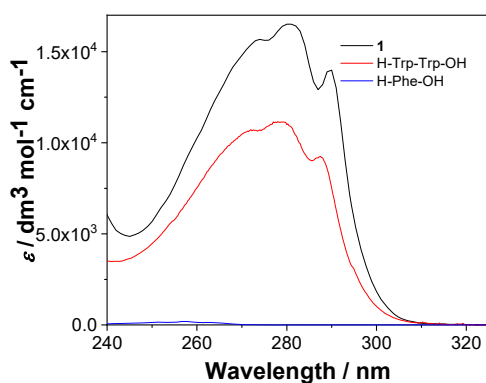


Fig. S2. Comparison of the absorptivity of **1** with the one of H-L-Trp-L-Trp-OH and H-L-Phe-OH from literature.⁴

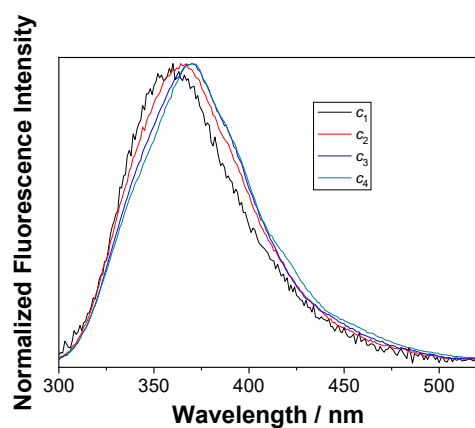


Fig. S3. Dependence of the normalized fluorescence spectra ($\lambda_{\text{ex}} = 280 \text{ nm}$) of **1** (5×10^{-7} - $2 \times 10^{-6} \text{ M}$), in aqueous solution in the presence of sodium cacodylate buffer (pH 7.0, 50 mM).

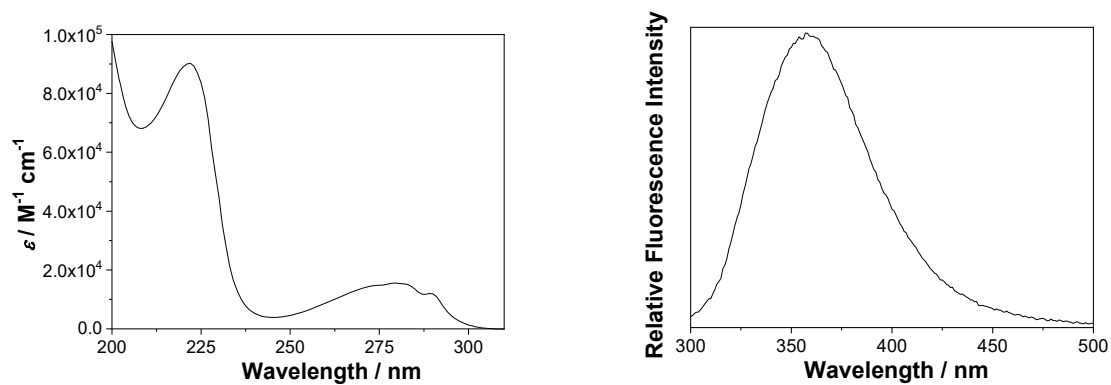


Fig. S4. Absorption spectrum (left) and emission spectrum ($\lambda_{\text{ex}} = 280$ nm) of **2** in CH_3CN .

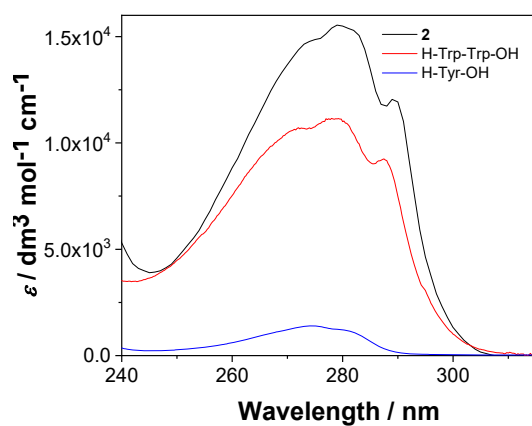


Fig. S5. Comparison of the absorptivity of **2** with the one of H-L-Trp-L-Trp-OH and H-L-Tyr-OH from literature.⁵

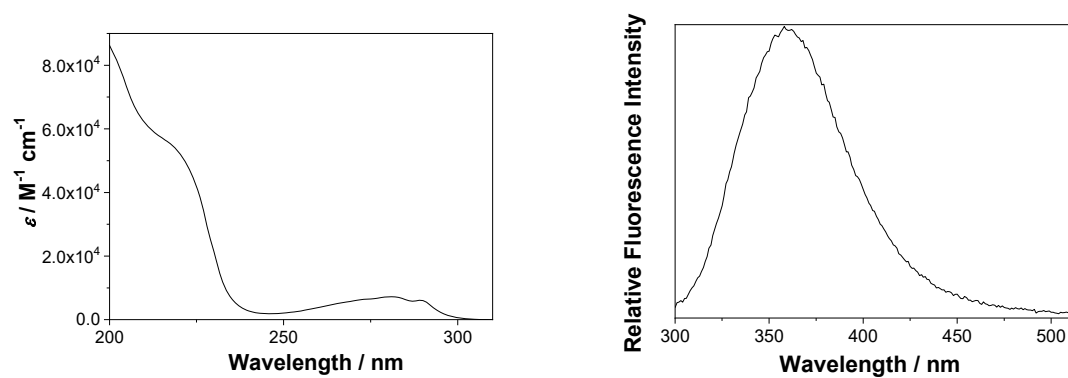


Fig. S6. Absorption spectrum (left) and emission spectrum ($\lambda_{\text{ex}} = 280$ nm) of **3** in CH_3CN .

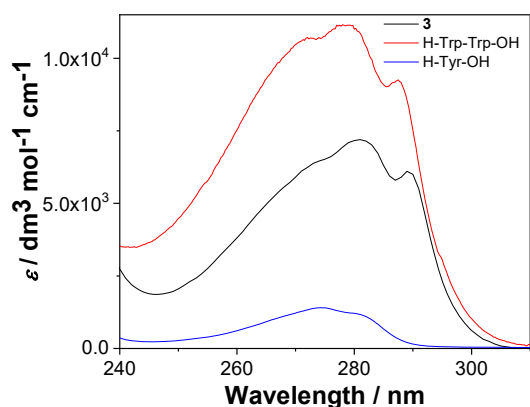


Fig. S7. Comparison of the absorptivity of **3** with the one of H-L-Trp-L-Trp-OH and H-L-Tyr-OH from literature.⁵

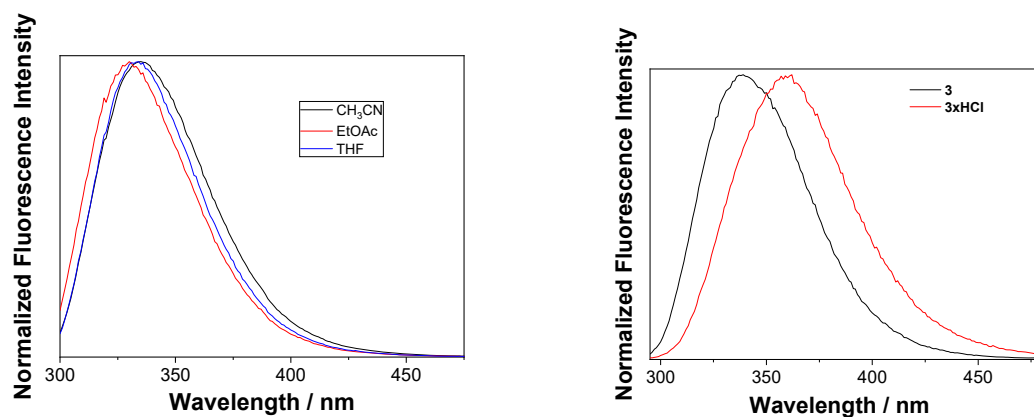


Fig. S8. Normalized fluorescence spectra ($\lambda_{\text{ex}} = 280$ nm) of **3** in CH₃CN, EtOAc and THF (left), and comparison of the fluorescence spectra of **3** in CH₃CN and **3**·HCl in CH₃CN-H₂O (1:9), sodium cacodilate buffer (50 mM, pH = 7.0).

Fluorescence quantum yield was calculated according to:

$$\Phi_f = \Phi_{\text{Ref}} \left(\frac{n}{n_R} \right)^2 \frac{I}{I_R} \frac{1-10^{-A_R}}{1-10^{-A}} \quad (\text{S6})$$

Φ_f and Φ_{Ref} – fluorescence quantum yield of compound and the reference;

n and n_R – refractive index of the solvent in which compound or the reference was dissolved;

A and A_R – absorbance of the compound and the reference at the excitation wavelength;

I and I_R – area under emission curve of the compound and the reference.

Fluorescence decays were obtained with time-correlated single-photon counting method on a FS5 Edinburgh Instruments spectrometer equipped for time correlated single photon counting method (TC-SPC). Pulsed LEDs at 280 nm was used for the excitation (pulse duration ≈ 800 ps). Fluorescence signals were monitored over 1023 channels with the time increment of ≈ 20 ps/channel. The decays were collected until they reached 3000 counts in the peak channel. The histograms were analyzed by a nonlinear least-squares deconvolution method using. The quality of the fit was judged by the reduced χ^2 being close to unity and the random distribution of the weighted residuals. Fluorescence decays were fit to a sum of exponentials using the following expression:

$$F(t) = \alpha_1 \exp\left(-\frac{t}{\tau_1}\right) + \alpha_2 \exp\left(-\frac{t}{\tau_2}\right) + \alpha_3 \exp\left(-\frac{t}{\tau_3}\right) + \dots \quad (\text{S7})$$

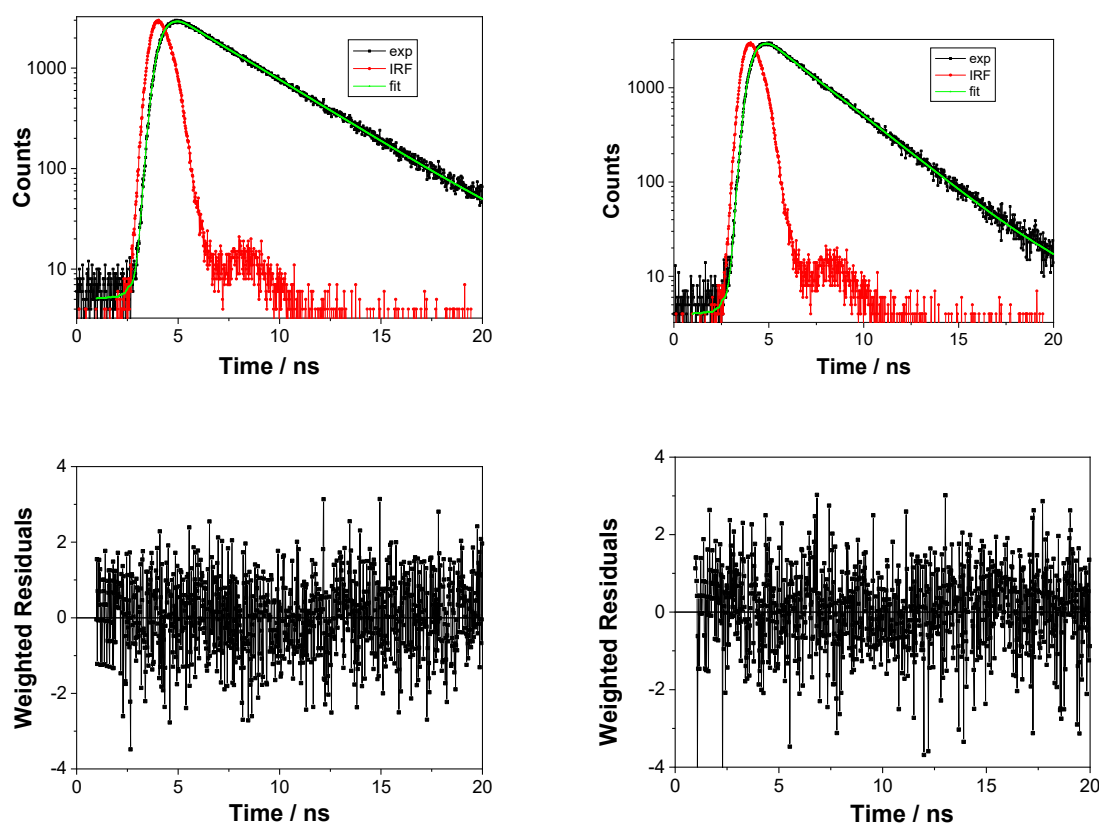


Fig. S9. Decay of fluorescence for **1** (left) and **2** (right) in CH₃CN at 370 nm upon excitation at 280 nm; bottom panels show weighted residuals between the experimental and fitted values.

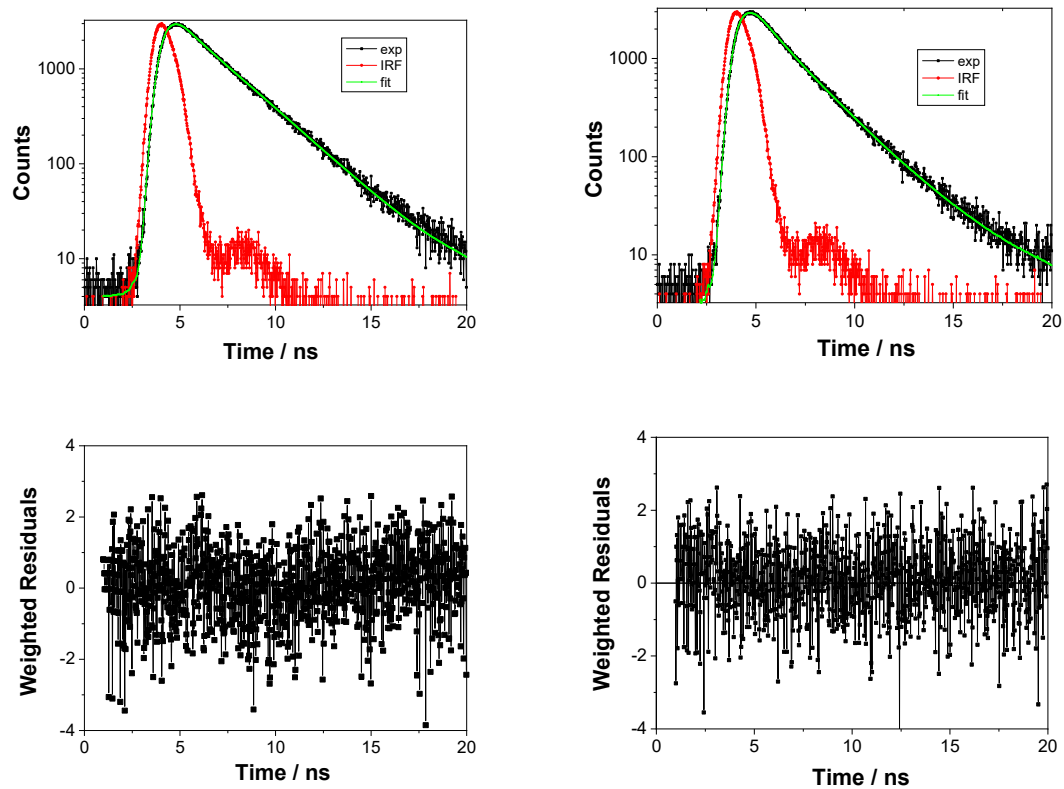


Fig. S10. Decay of fluorescence for **3** (left) in CH₃CN and **3**×HCl (right) in CH₃CN-H₂O (1:9) at 370 nm upon excitation at 280 nm; bottom panels show weighted residuals between the experimental and fitted values.

3. Laser Flash Photolysis

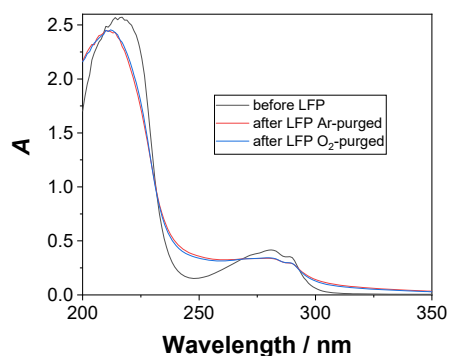


Fig. S11. UV-vis spectra of tripeptide **3** in CH₃CN ($c = 6.1 \times 10^{-5}$ M) before and after the LFP experiment.

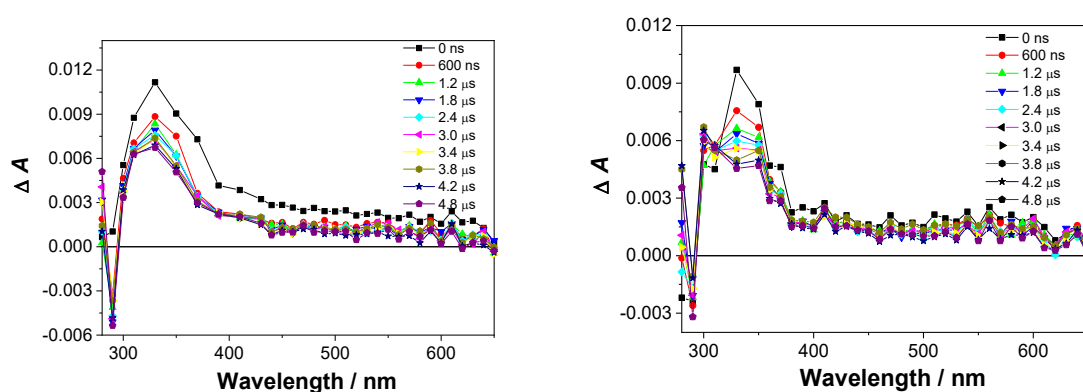


Fig. S12. Transient absorption spectra of Ar-purged (left) and O₂-purged (right) solution of **3** in CH₃CN ($c = 6.1 \times 10^{-5}$ M), excited at 266 nm, $A_{266} = 0.28$, laser power ≈ 18 mJ/pulse.

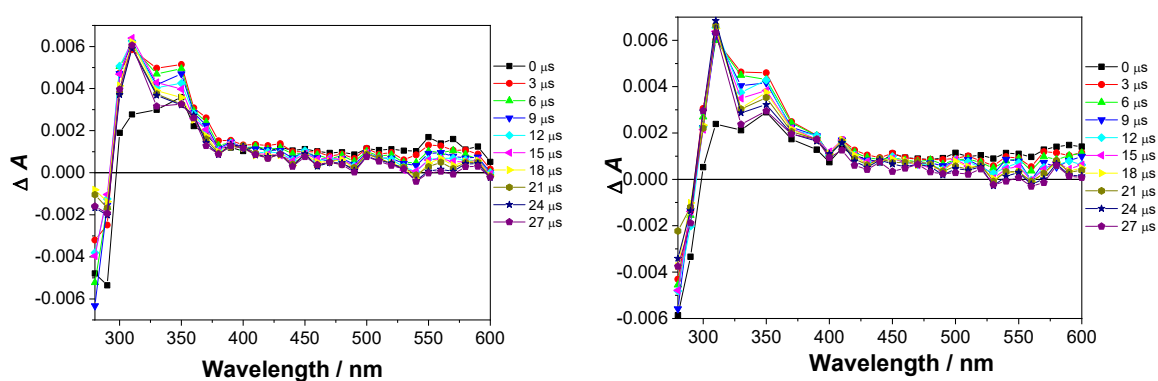


Fig. S13. Transient absorption spectra of Ar-purged (left) and O₂-purged (right) solution of **3** in CH₃CN ($c = 6.1 \times 10^{-5}$ M), excited at 266 nm, $A_{266} = 0.28$, laser power ≈ 18 mJ/pulse.

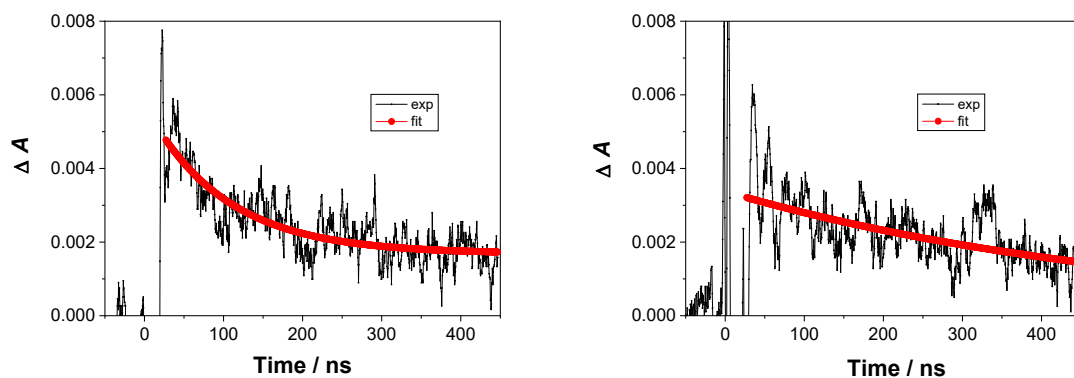


Fig. S14. Decay of transient absorption at 380 nm for Ar-purged (left) and O₂-purged (right) solution of **3** in CH₃CN ($c = 6.1 \times 10^{-5}$ M), excited at 266 nm, $A_{266} = 0.28$.

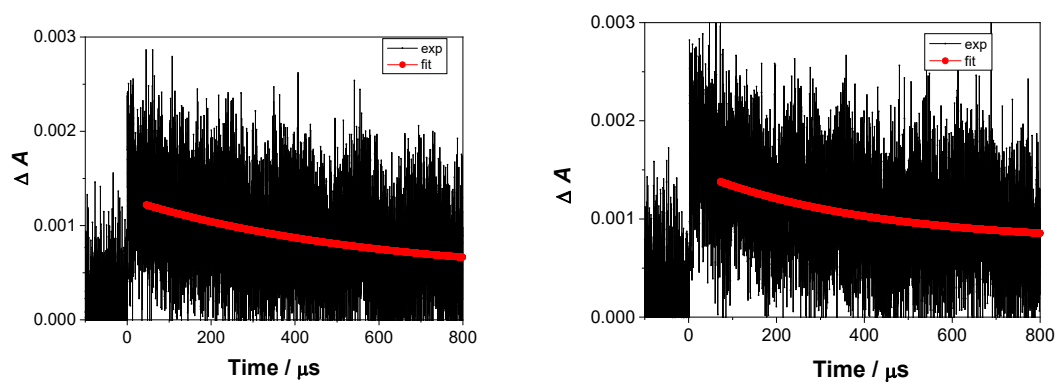


Fig. S15. Decay of transient absorption at 380 nm for Ar-purged (left) and O₂-purged (right) solution of **3** in CH₃CN ($c = 6.1 \times 10^{-5}$ M), excited at 266 nm, $A_{266} = 0.28$.

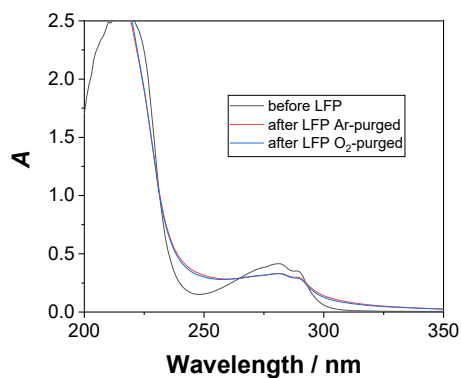


Fig. S16. UV-vis spectra of tripeptide **3** ($c = 6.1 \times 10^{-5}$ M) in CH₃CN-H₂O (1:1 v/v, in the presence of phosphate buffer $c = 50$ mM, pH = 7.0) before and after the LFP experiment.

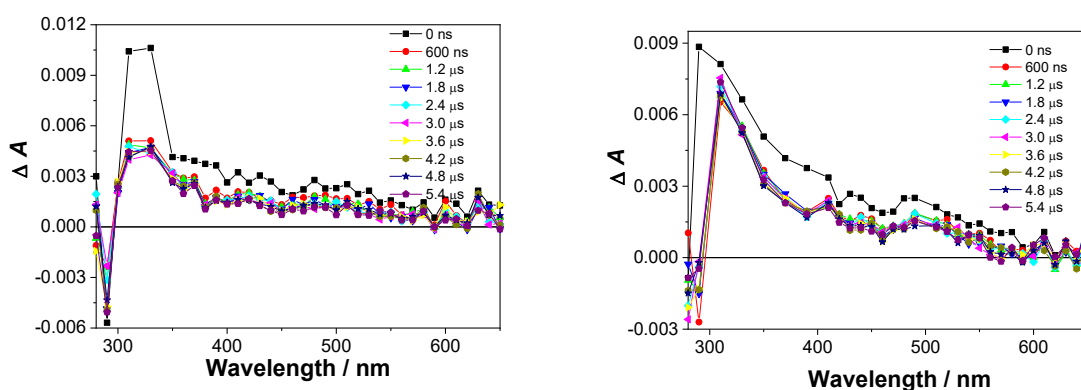


Fig. S17. Transient absorption spectra of Ar-purged (left) and O₂-purged (right) solution of **3** ($c = 6.1 \times 10^{-5}$ M) in CH₃CN-H₂O (1:1 v/v, in the presence of phosphate buffer $c = 50$ mM, pH = 7.0), excited at 266 nm, $A_{266} = 0.30$, laser power ≈ 18 -19 mJ/pulse.

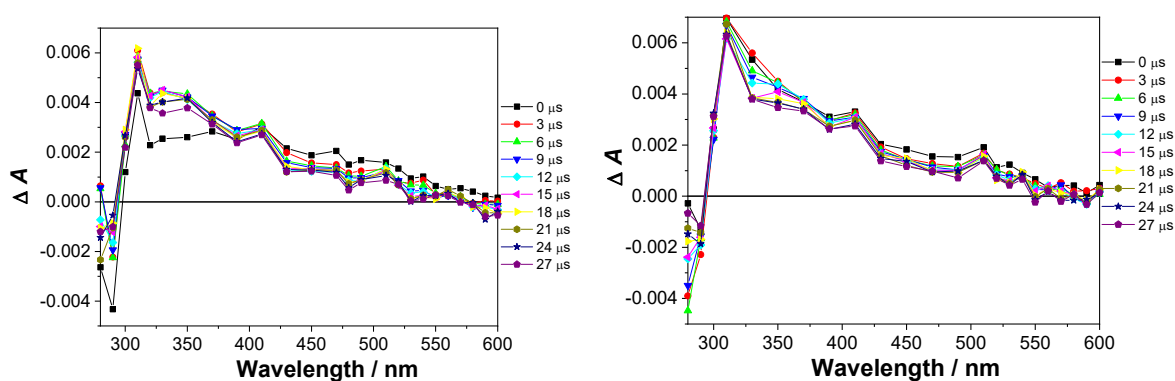


Fig. S18. Transient absorption spectra of Ar-purged (left) and O₂-purged (right) solution of **3** ($c = 6.1 \times 10^{-5}$ M) in CH₃CN-H₂O (1:1 v/v, in the presence of phosphate buffer $c = 50$ mM, pH = 7.0), excited at 266 nm, $A_{266} = 0.30$, laser power 18-19 mJ/pulse.

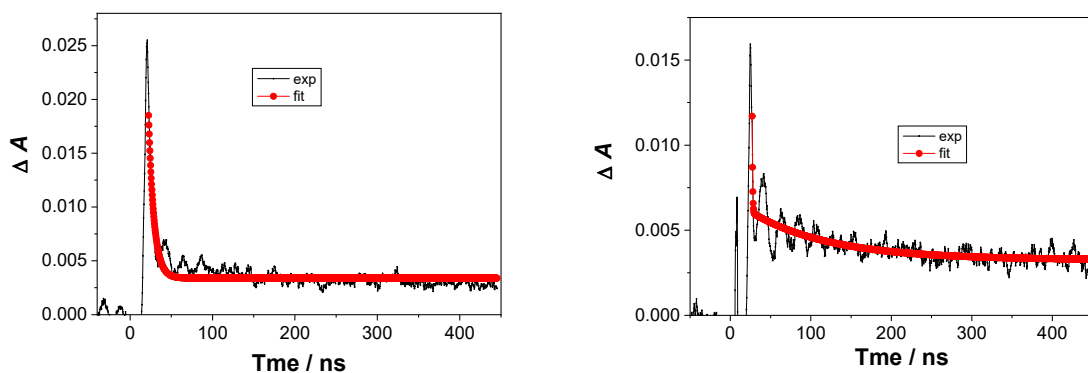


Fig. S19. Decay of transient absorption at 400 nm for Ar-purged (left) and O₂-purged (right) solution of **3** ($c = 6.1 \times 10^{-5}$ M) in CH₃CN-H₂O (1:1 v/v, in the presence of phosphate buffer $c = 50$ mM, pH = 7.0), excited at 266 nm, $A_{266} = 0.30$.

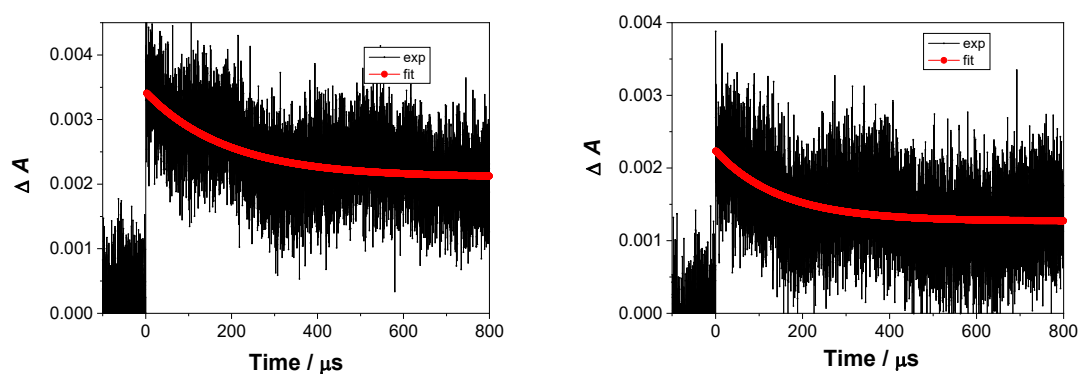


Fig. S20. Decay of transient absorption at 380 nm for Ar-purged (left) and O₂-purged (right) solution of **3** ($c = 6.1 \times 10^{-5}$ M) in CH₃CN-H₂O (1:1 v/v, in the presence of phosphate buffer $c = 50$ mM, pH = 7.0), excited at 266 nm, $A_{266} = 0.30$.

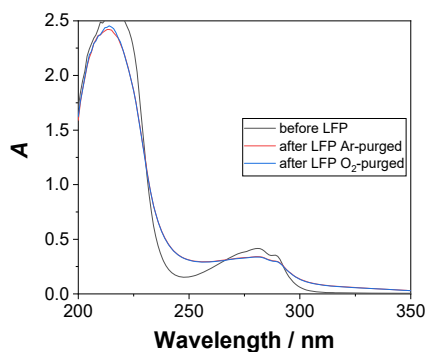


Fig. S21. UV-vis spectra of tripeptide **3**×HCl ($c = 9.5 \times 10^{-5}$ M) in CH₃CN-H₂O (1:1 v/v, in the presence of phosphate buffer $c = 50$ mM, pH = 7.0) before and after the LFP experiment.

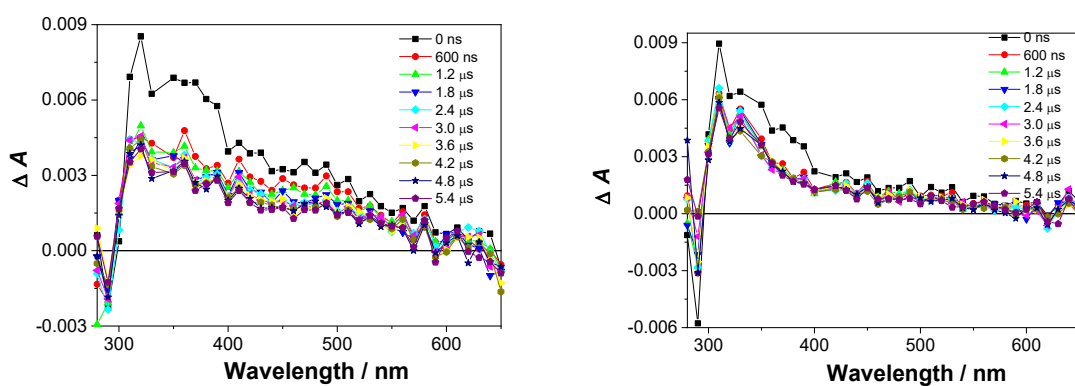


Fig. S22. Transient absorption spectra of Ar-purged (left) and O₂-purged (right) solution of **3**×HCl ($c = 9.5 \times 10^{-5}$ M) in CH₃CN-H₂O (1:1 v/v, in the presence of phosphate buffer $c = 50$ mM, pH = 7.0), excited at 266 nm, $A_{266} = 0.30$, laser power ≈ 19 mJ/pulse.

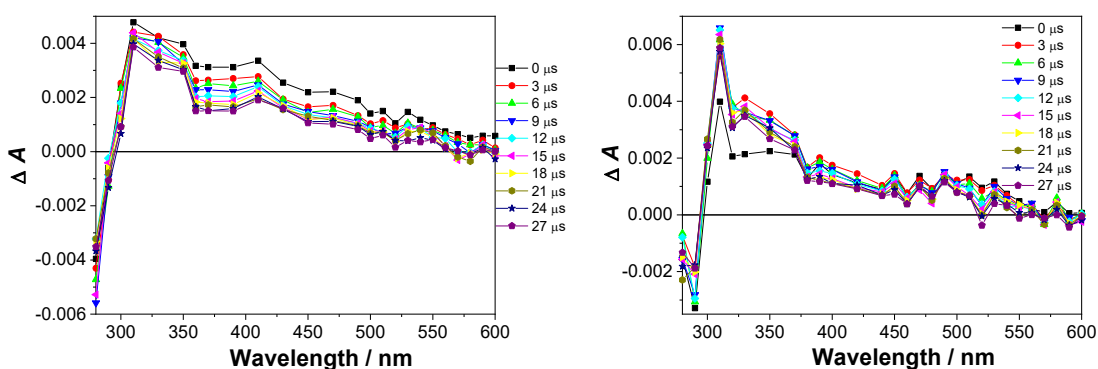


Fig. S23. Transient absorption spectra of Ar-purged (left) and O₂-purged (right) solution of **3**×HCl ($c = 9.5 \times 10^{-5}$ M) in CH₃CN-H₂O (1:1 v/v, in the presence of phosphate buffer $c = 50$ mM, pH = 7.0), excited at 266 nm, $A_{266} = 0.30$, laser power ≈ 19 mJ/pulse.

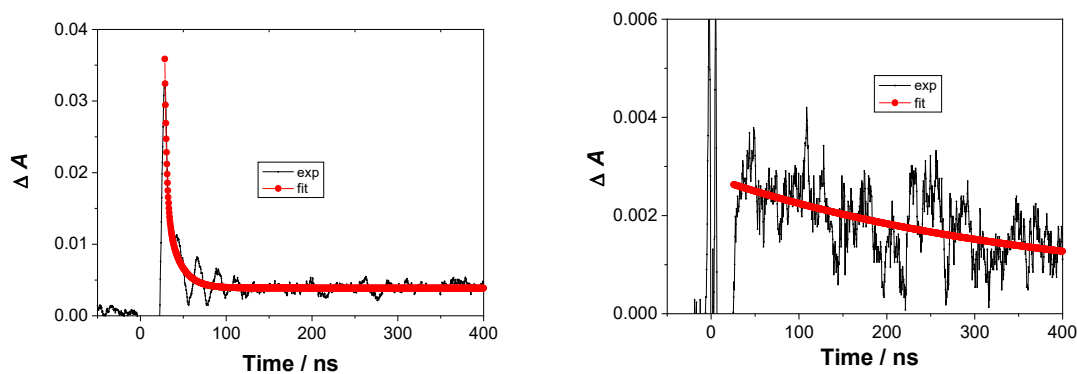


Fig. S24. Decay of transient absorption at 380 nm for Ar-purged (left) and O₂-purged (right) solution of **3**×HCl ($c = 9.5 \times 10^{-5}$ M) in CH₃CN-H₂O (1:1 v/v, in the presence of phosphate buffer $c = 50$ mM, pH = 7.0), excited at 266 nm, $A_{266} = 0.30$, laser power ≈ 19 mJ/pulse.

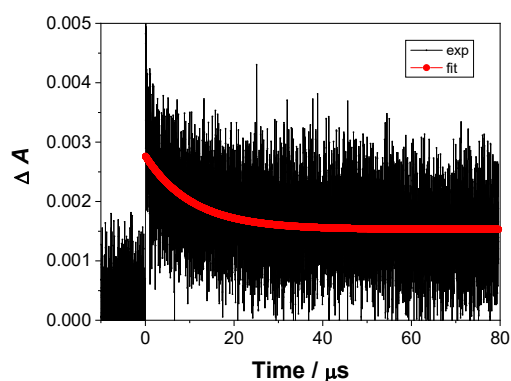


Fig. S25. Decay of transient absorption at 400 nm for Ar-purged solution of ($c = 9.5 \times 10^{-5}$ M) in CH₃CN-H₂O (1:1 v/v, in the presence of phosphate buffer $c = 50$ mM, pH = 7.0), excited at 266 nm, $A_{266} = 0.30$, laser power ≈ 19 mJ/pulse.

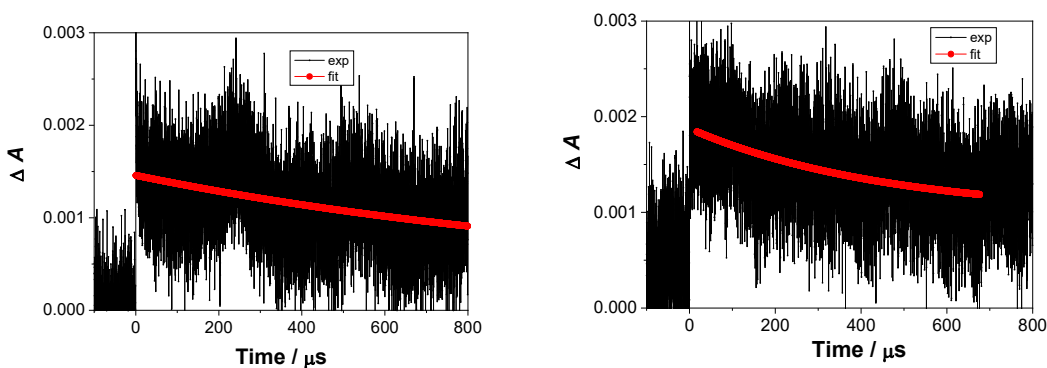


Fig. S26. Decay of transient absorption at 400 nm for Ar-purged (left) and O₂-purged (right) solution of **3**×HCl ($c = 9.5 \times 10^{-5}$ M) in CH₃CN-H₂O (1:1 v/v, in the presence of phosphate buffer $c = 50$ mM, pH = 7.0), excited at 266 nm, $A_{266} = 0.30$, laser power ≈ 19 mJ/pulse.

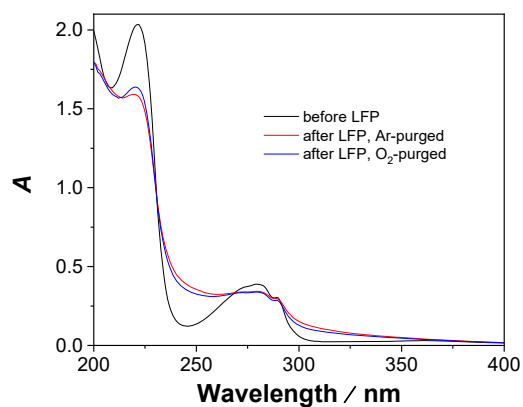


Fig. S27. UV-vis spectra of tripeptide **2** in CH₃CN ($c = 2.95 \times 10^{-5}$ M) before and after the LFP experiment.

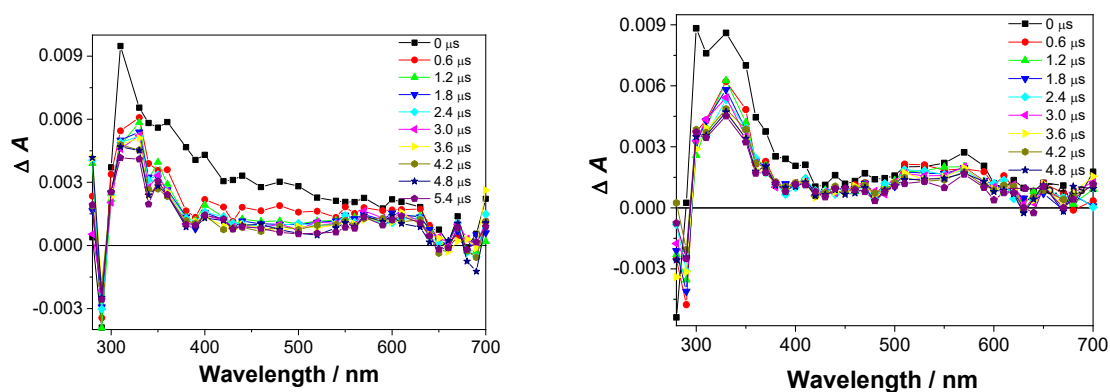


Fig. S28. Transient absorption spectra of Ar-purged (left) and O₂-purged (right) solution of **2** in CH₃CN ($c = 2.95 \times 10^{-5}$ M), excited at 266 nm, $A_{266} = 0.31$, laser power ≈ 19 mJ/pulse.

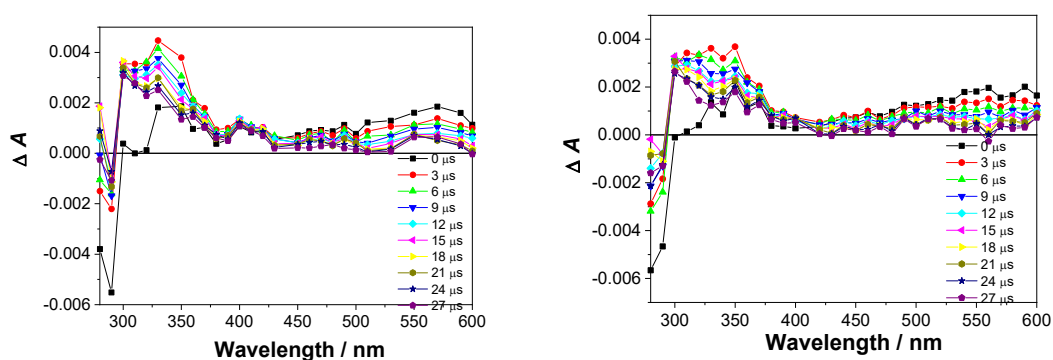


Fig. S29. Transient absorption spectra of Ar-purged (left) and O₂-purged (right) solution of **2** in CH₃CN ($c = 2.95 \times 10^{-5}$ M), excited at 266 nm, $A_{266} = 0.31$, laser power ≈ 19 mJ/pulse.

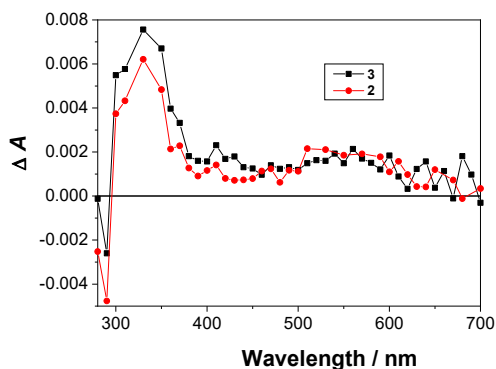


Fig. S30. Transient absorption spectra of optically matched ($A_{266} = 0.30$) O_2 -purged solution of **3** in CH_3CN ($c = 6.1 \times 10^{-5}$ M) and **2** in CH_3CN ($c = 2.95 \times 10^{-5}$ M). The spectra were measured with a delay of 600 ns, laser power ≈ 19 mJ/pulse.

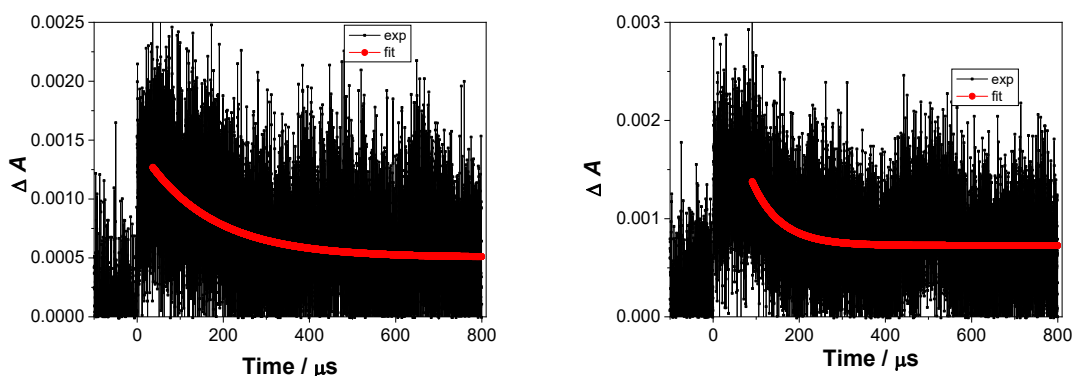


Fig. S31. Decay of transient absorption at 380 nm for Ar-purged (left) and O_2 -purged (right) solution of **2** in CH_3CN ($c = 2.95 \times 10^{-5}$ M), excited at 266 nm, $A_{266} = 0.28$.

In the Ar-purged CH_3CN solution of **2** we detected several transients with the lifetimes of 23 ± 2 ns, 1.1 ± 0.1 μ s, 13 ± 1 μ s and 120 ± 40 μ s. In the O_2 -purged solution we detected transients with lifetimes 19 ± 1 ns, 12 ± 2 μ s and 55 ± 10 μ s. The transient with the lifetime of 1.1 μ s may therefore be assigned to the triplet excited state. The other transients were not assigned. A very long-lived transient, which was detected from **3** and tentatively assigned to QM here was not detected. Additional transient was detected at $\lambda > 500$ nm with $\tau \approx 9$ -12 μ s, that was not quenched by O_2 . It was tentatively assigned to Trp radical-cation, since it was not detected in the aqueous solvent (vide infra), and based on the literature precedent.

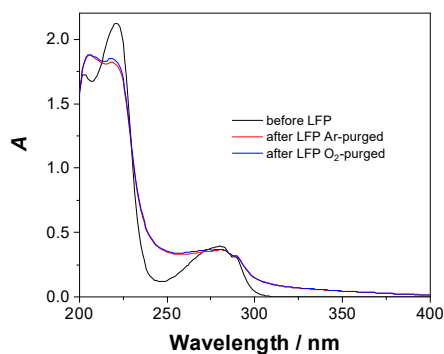


Fig. S32. UV-vis spectra of tripeptide **2** ($c = 3.2 \times 10^{-5}$ M) in CH₃CN-H₂O (1:1 v/v, in the presence of phosphate buffer $c = 50$ mM, pH = 7.0) before and after the LFP experiment.

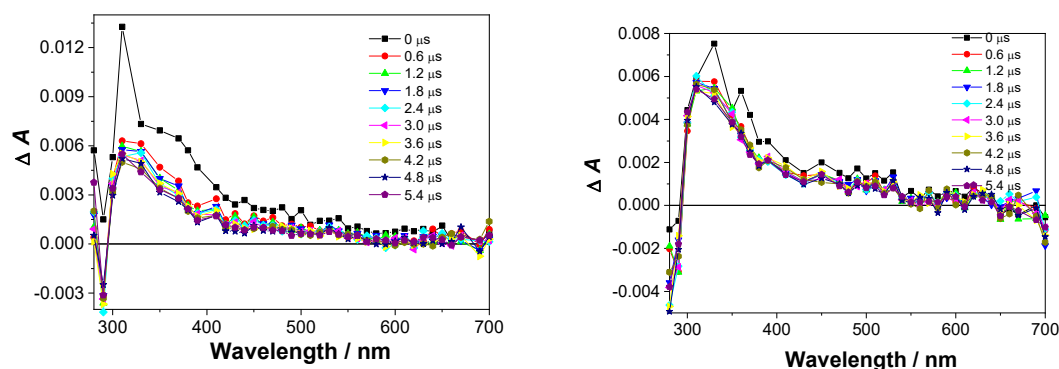


Fig. S33. Transient absorption spectra of Ar-purged (left) and O₂-purged (right) solution of **2** ($c = 3.2 \times 10^{-5}$ M) in CH₃CN-H₂O (1:1 v/v, in the presence of phosphate buffer $c = 50$ mM, pH = 7.0), excited at 266 nm, $A_{266} = 0.30$, laser power ≈ 18 mJ/pulse.

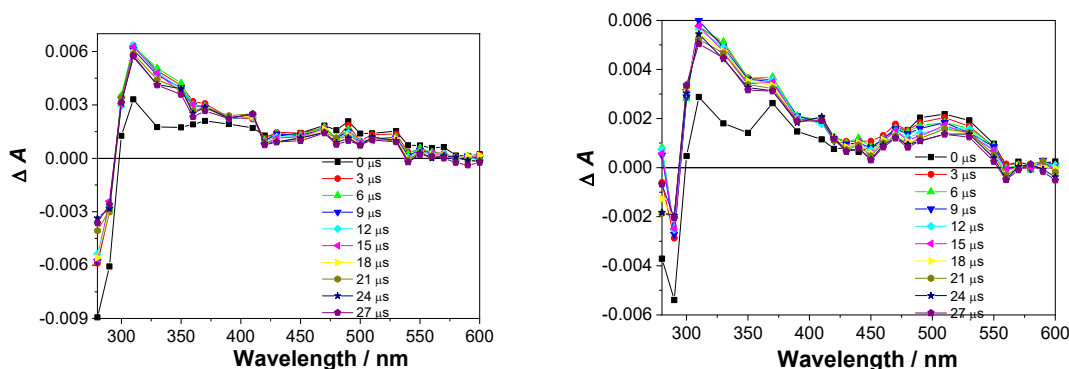


Fig. S34. Transient absorption spectra of Ar-purged (left) and O₂-purged (right) solution of **2** ($c = 3.2 \times 10^{-5}$ M) in CH₃CN-H₂O (1:1 v/v, in the presence of phosphate buffer $c = 50$ mM, pH = 7.0), excited at 266 nm, $A_{266} = 0.30$, laser power ≈ 18 mJ/pulse.

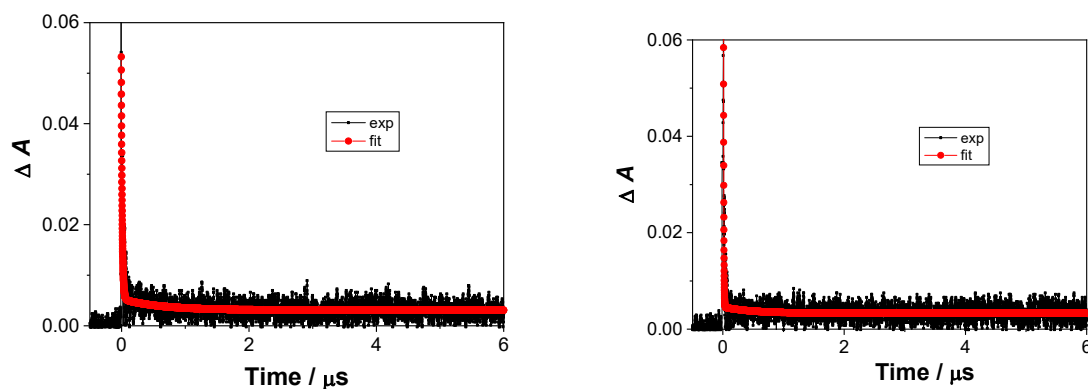


Fig. S35. Decay of transient absorption at 360 nm for Ar-purged (left) and O₂-purged (right) solution of **2** ($c = 3.2 \times 10^{-5}$ M) in CH₃CN-H₂O (1:1 v/v, in the presence of phosphate buffer $c = 50$ mM, pH = 7.0), $A_{266} = 0.30$, laser power ≈ 18 mJ/pulse.

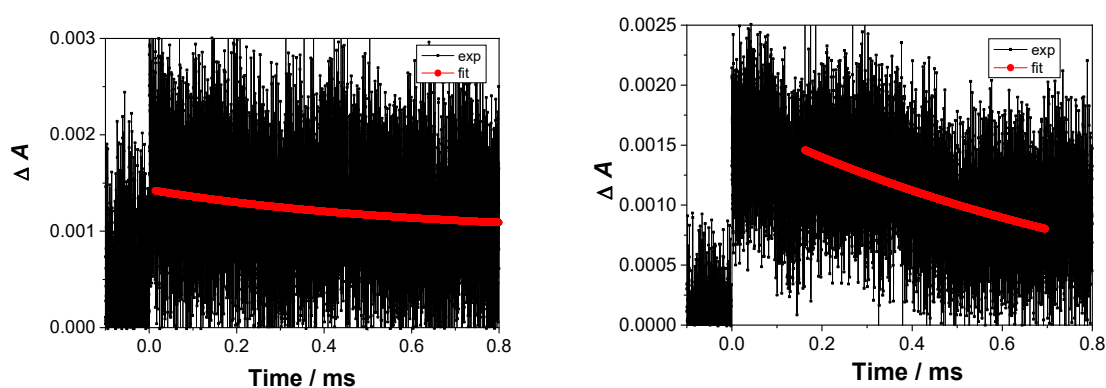


Fig. S36. Decay of transient absorption at 360 nm for Ar-purged (left) and O₂-purged (right) solution of **2** ($c = 3.2 \times 10^{-5}$ M) in CH₃CN-H₂O (1:1 v/v, in the presence of phosphate buffer $c = 50$ mM, pH = 7.0), $A_{266} = 0.30$, laser power ≈ 18 mJ/pulse.

In the Ar-purged CH₃CN-H₂O solution of **2** we detected several transients with the lifetimes of 14 ± 3 ns, 500 ± 100 ns, 13 ± 1 μ s and 600 ± 300 μ s, and none of the transients was quenched by O₂. Thus, in the O₂-purged solution, similar transients were detected with lifetimes 15 ± 5 ns, 1.1 ± 0.1 μ s and 900 ± 500 μ s. The transients at $\lambda > 500$ nm were not detected, in agreement with their assignment to Trp radical cation which in aqueous solution very readily deprotonates to the *N*-centered radical, for which quenching by O₂ is also not anticipated. Thus, the long-lived transient can plausibly be assigned to the Trp radical. Due to concomitant formation of Trp radical and **QM-3** the detection of **3** was more difficult and the spectra of **2** and **3** in aqueous solution are more similar (Fig S35).

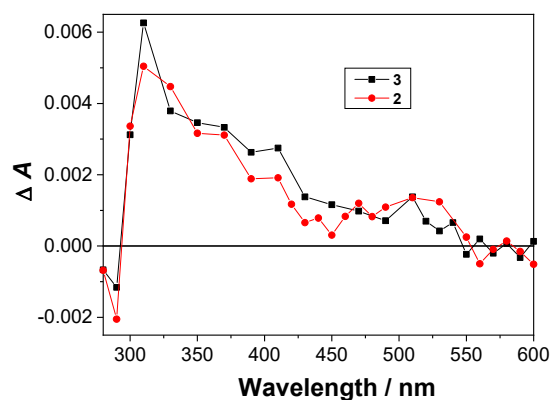


Fig. S37. Transient absorption spectra of optically matched ($A_{266} = 0.30$) O_2 -purged solution of **3** ($c = 6.1 \times 10^{-5}$ M) and **2** ($c = 3.2 \times 10^{-5}$ M) in CH_3CN-H_2O (1:1 v/v, in the presence of phosphate buffer $c = 50$ mM, pH = 7.0). The spectra were measured 600 ns after the laser pulse at 266 nm, laser power ≈ 19 mJ/pulse.

4. Noncovalent binding to polynucleotides

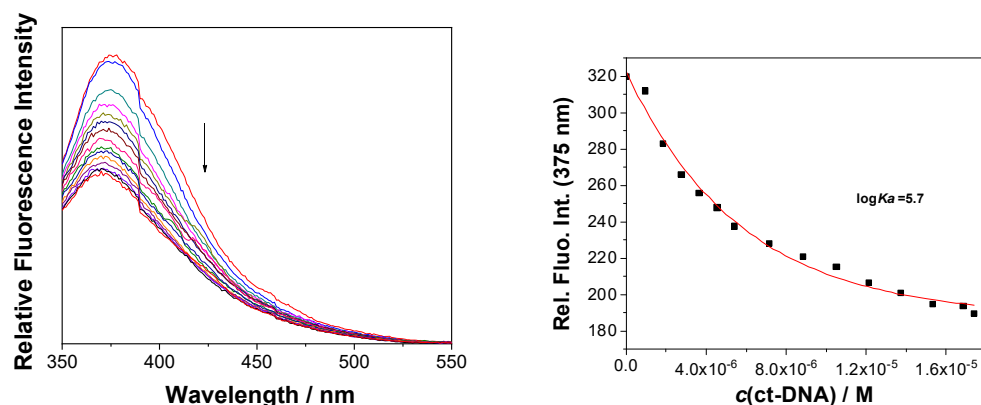


Fig. S38. Left: Fluorescence titration of **1**×HCl ($c = 3.3 \times 10^{-6}$ M, $\lambda_{\text{exc}} = 300$ nm) with ct-DNA ($c = 1.2 \times 10^{-6}$ - 6.7×10^{-5} M); in cacodylate buffer (pH 7.0, 50 mM at 25 °C) with 20% DMSO. Right: Dependence of the fluorescence intensity at 375 nm on the ct-DNA concentration; dots are experimental values and the red line is calculated fit according to the Scatchard model.

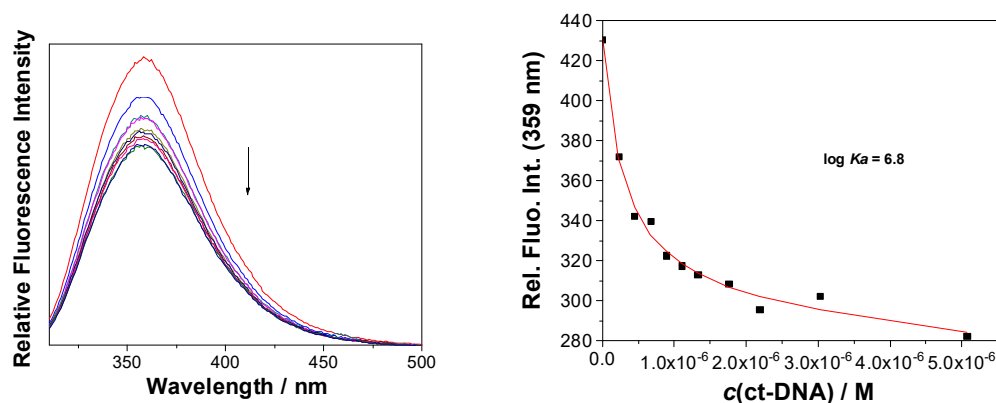


Fig. S39. Left: Fluorescence titration of **2**×HCl ($c = 2.4 \times 10^{-6}$ M, $\lambda_{\text{exc}} = 295$ nm) with ct-DNA ($c = 1.2 \times 10^{-6}$ - 6.7×10^{-5} M); in cacodylate buffer (pH 7.0, 50 mM at 25 °C) with 20% DMSO. Right: Dependence of the fluorescence intensity at 359 nm on the ct-DNA concentration; dots are experimental values and the red line is calculated fit according to the Scatchard model.

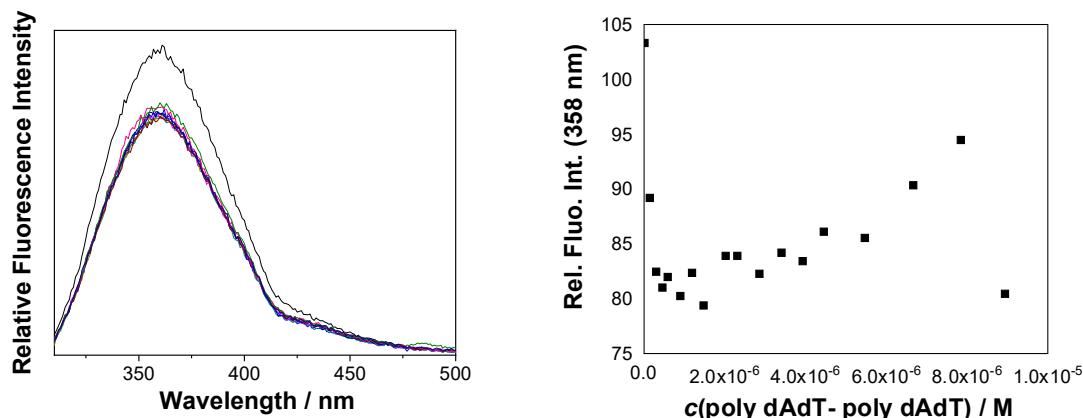


Fig. S40. Fluorescence titration of **2xHCl** ($c = 3.9 \times 10^{-6}$ M, $\lambda_{\text{exc}} = 295$ nm) with poly dAdT - poly dAdT in cacodylate buffer (pH 7.0, 50 mM at 25 °C). Small emission changes in opposite directions (quenching at $r[\text{dye}]/[\text{DNA}] > 1$ and emission increase for $r < 0.5$) did not allow processing of data by Scatchard model.

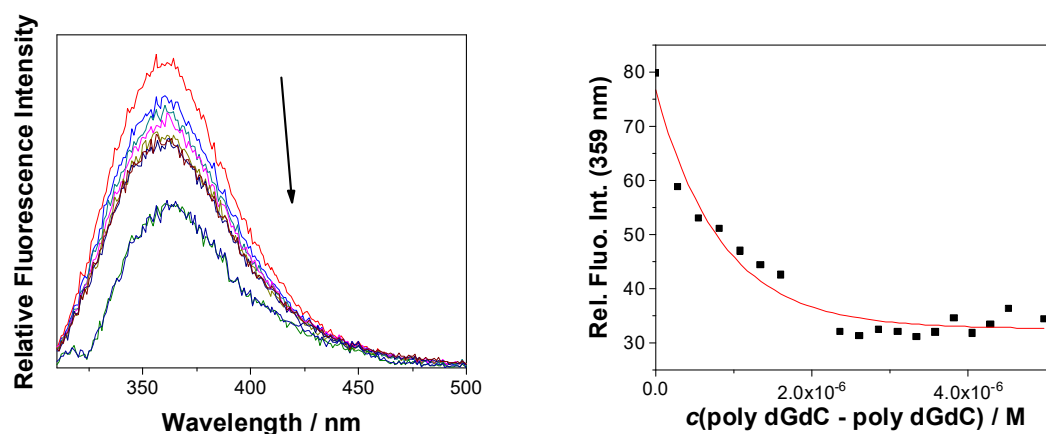


Fig. S41. LEFT: Fluorescence titration of **2xHCl** ($c = 3.0 \times 10^{-6}$ M, $\lambda_{\text{exc}} = 295$ nm) with poly dGdC - poly dGdC in cacodylate buffer (pH 7.0, 50 mM at 25 °C); RIGHT: dependence of the fluorescence intensity (normalized to starting emission) at $\lambda_{\text{em}} = 359$ nm on the $c(\text{polynucleotide})$, dots are experimental values and the line represents calculated fit to the Scatchard model, with the fixed value of $n = [\text{bound } \mathbf{2xHCl}]/[\text{polynucleotide}] = 0.3$.

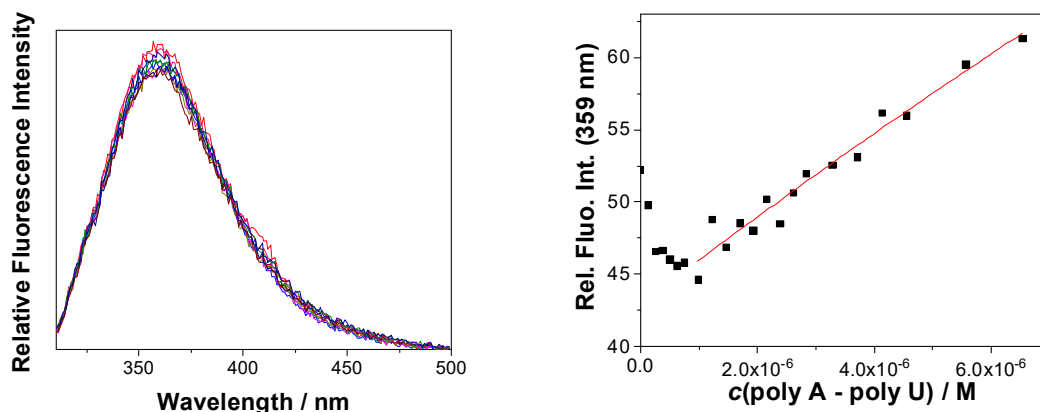


Fig. S42. LEFT: Fluorescence titration of **2xHCl** ($c = 3.0 \times 10^{-6}$ M, $\lambda_{\text{exc}} = 295$ nm) with poly A - poly U in cacodylate buffer (pH 7.0, 50 mM at 25 °C); RIGHT: dependence of the fluorescence intensity (normalized to starting emission) at $\lambda_{\text{em}} = 359$ nm on the $c(\text{polynucleotide})$, dots are experimental values and the lines represent calculated fit to the Scatchard model, with the fixed value of $n = [\text{bound } \mathbf{2xHCl}] / [\text{polynucleotide}] = 0.3$.

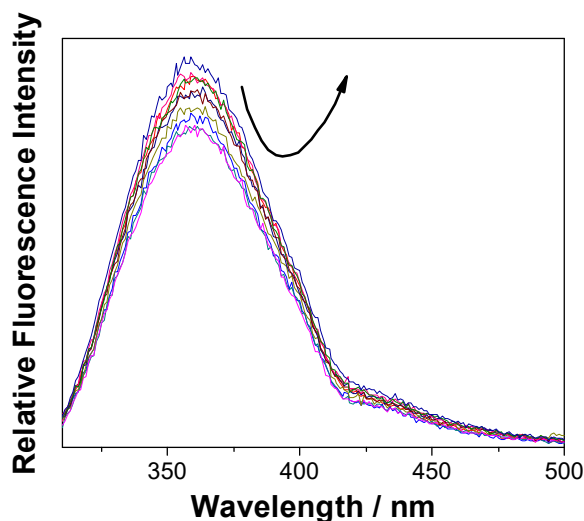


Fig. S43. Fluorescence titration of **3xHCl** ($c = 3.0 \times 10^{-6}$ M, $\lambda_{\text{exc}} = 295$ nm) with poly dAdT – poly dAdT in cacodylate buffer (pH 7.0, 50 mM at 25 °C); dependence of the fluorescence intensity at $\lambda_{\text{em}} = 380$ nm (normalized to starting emission) on the $c(\text{polynucleotide})$ is shown in Fig. 3.

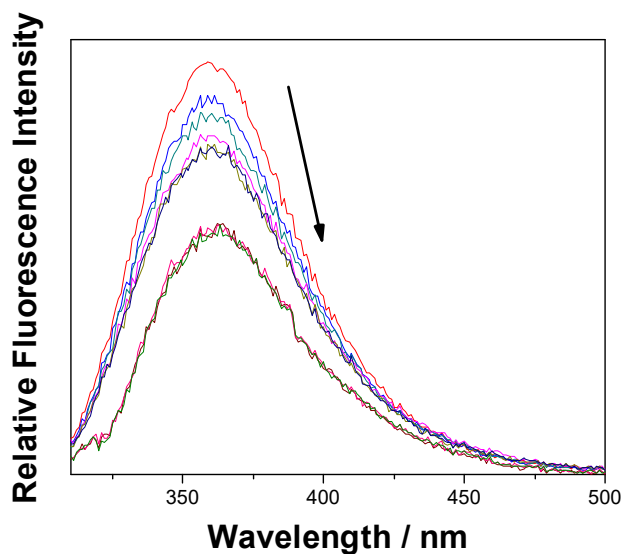


Fig. S44. Fluorescence titration of $3\times\text{HCl}$ ($c = 3.0\times 10^{-6}$ M, $\lambda_{\text{exc}} = 295$ nm) with poly dGdC – poly dGdC in cacodylate buffer (pH 7.0, 50 mM at 25 °C); dependence of the fluorescence intensity at $\lambda_{\text{em}} = 380$ nm (normalized to starting emission) on the $c(\text{polynucleotide})$ is shown in Fig. 3.

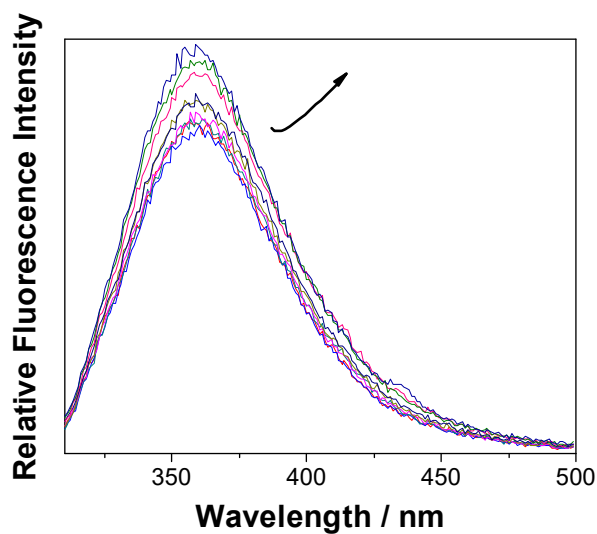


Fig. S45. Fluorescence titration of $3\times\text{HCl}$ ($c = 3.0\times 10^{-6}\text{mol dm}^{-3}$, $\lambda_{\text{exc}} = 295$ nm) with poly A – poly U in cacodylate buffer (pH 7.0, 50 mM at 25 °C); dependence of the fluorescence intensity at $\lambda_{\text{em}} = 380$ nm (normalized to starting emission) on the $c(\text{polynucleotide})$ shown in Fig. 3. Done in cacodylate buffer (pH 7.0, $I=50$ mM, at 25 °C).

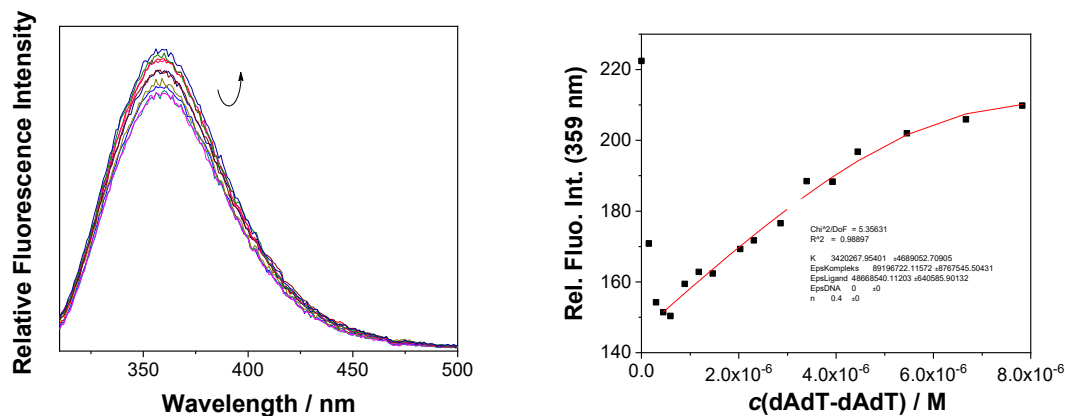


Fig. S46. Left: Fluorimetric titration of $3\times\text{HCl}$ ($c = 3.0\times 10^{-6}$ M, $\lambda_{\text{exc}} = 280$ nm) with poly dAdT - poly dAdT ($c = 1.2\times 10^{-6}$ - 6.7×10^{-5} M); in cacodylate buffer (pH 7.0, 50 mM, at 25 °C). Right: Dependence of the fluorescence intensity at 359 nm on the polynucleotide concentration; dots are experimental values and the red line is calculated fit according to the Scatchard model, with the fixed value of $n = [3\times\text{HCl}]/[\text{dAdT}] = 0.4$.

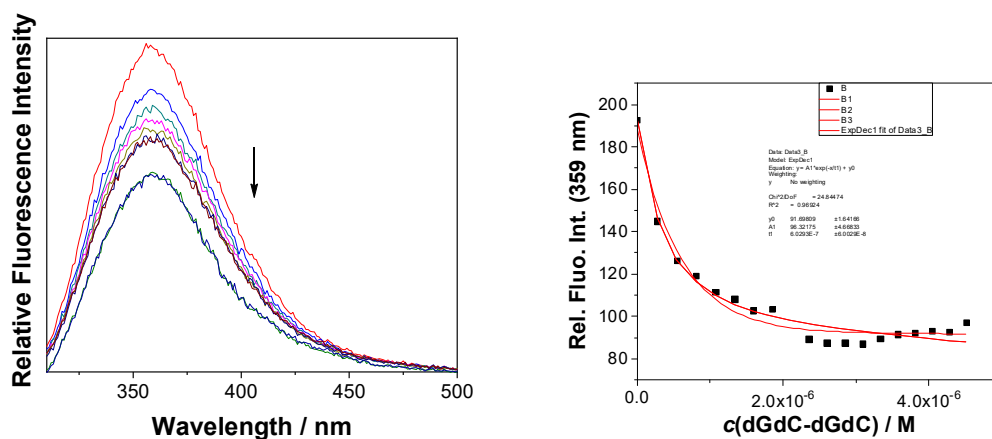


Fig. S47. Left: Fluorimetric titration of $3\times\text{HCl}$ ($c = 3.0\times 10^{-6}$ M, $\lambda_{\text{exc}} = 280$ nm) with poly dGdC - poly dGdC ($c = 1.2\times 10^{-6}$ - 6.7×10^{-5} M); in cacodylate buffer (pH 7.0, 50 mM, at 25 °C). Right: Dependence of the fluorescence intensity at 359 nm on the polynucleotide concentration; dots are experimental values and the red line is calculated fit according to the Scatchard model. Data could not be fit to the model with the fixed value of $n = [3\times\text{HCl}]/[\text{dAdT}] < 1$.

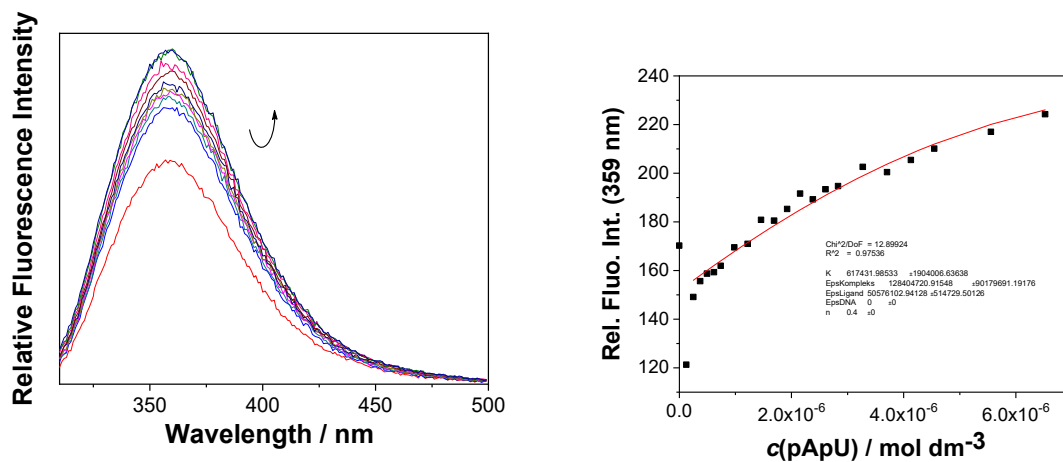


Fig. S48. Left: Fluorimetric titration of $\mathbf{3} \times \text{HCl}$ ($c = 3.0 \times 10^{-6} \text{ M}$, $\lambda_{\text{exc}} = 280 \text{ nm}$) with polyA-poly U ($c = 1.2 \times 10^{-6} - 6.7 \times 10^{-5} \text{ M}$); in cacodylate buffer (pH 7.0, 50 mM, at 25°C). Right: Dependence of the fluorescence intensity at 359 nm on the poly A – poly U concentration; dots are experimental values and the red line is calculated fit according to the Scatchard model with the fixed value of $n = [\mathbf{3} \times \text{HCl}]/[\text{poly A – poly U}] = 0.4$.

The effect to the polynucleotide melting temperature is defined as:

$$\Delta T_m = T_m (\text{complex}) - T_m (\text{ct-DNA}) \quad (\text{S8})$$

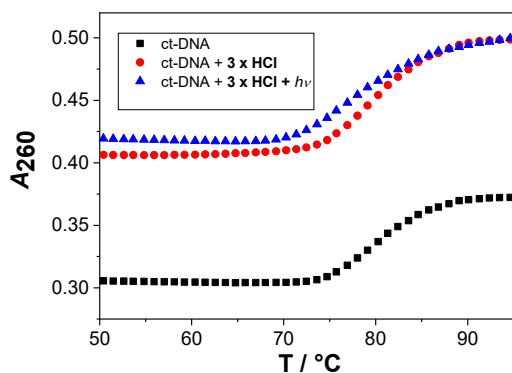


Fig. S49. Thermal denaturation of ct-DNA ($c = 3 \times 10^{-5}$ M), in the presence of **3**×**HCl** at ratio $r[\mathbf{3} \times \mathbf{HCl}] / [\text{polynucleotide}] = 0.3$, at pH = 7.0, cacodylate buffer (50 mM), and after irradiation of ct-DNA and **3** (300 nm, 5 min).

Table S3. The ΔT_m values^a of ct-DNA upon the addition of **3**×**HCl** at pH 7.0 (sodium cacodylate buffer, $I = 0.05$ M) and upon irradiation (300 nm, 8 lamps, 5 min).

Compound/condition	$\Delta T_m / ^\circ\text{C}$
3 × HCl (dark)	0.5
3 × HCl + $h\nu$	-2.2

^a Error in $\Delta T_m : \pm 0.5^\circ\text{C}$; The melting temperature was determined from the inflection point of the dependence of absorbance on temperature.^[6] $r[\mathbf{3} \times \mathbf{HCl}] / [\text{ct-DNA}] = 0.3$.

CD experiments

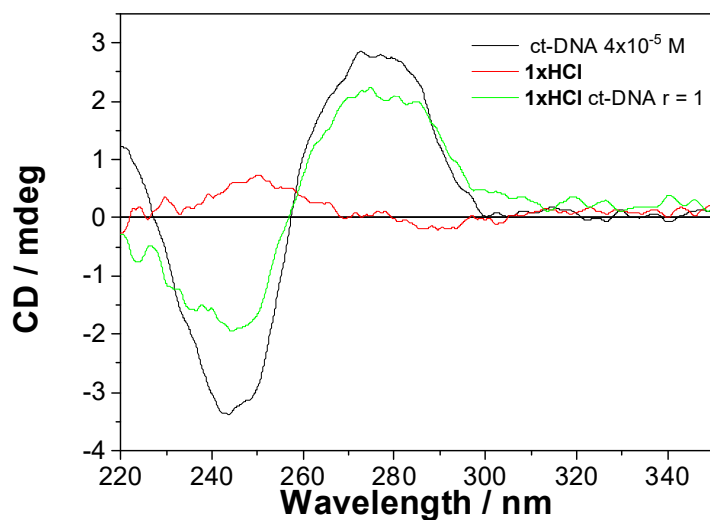


Fig. S50. CD spectra of ct-DNA ($c = 4.0 \times 10^{-5}$ M), **1xHCl** and their mixture at $r[\mathbf{1xHCl}]/[\text{ct-DNA}] = 1$. The measurement was performed in cacodylate buffer / 20% DMSO (pH 7.0, 50 mM, at 25 °C).

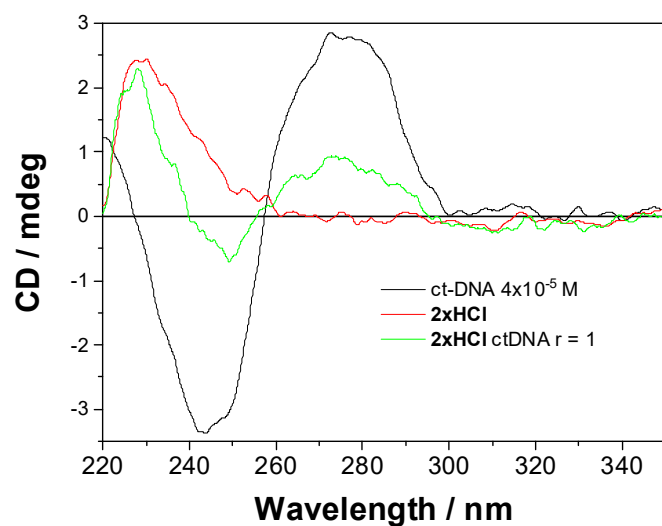


Fig. S51. CD spectra of ct-DNA ($c = 4.0 \times 10^{-5}$ M), **2xHCl** and their mixture at $r[\mathbf{2xHCl}]/[\text{ct-DNA}] = 1$. The measurement was performed in cacodylate buffer / 20% DMSO (pH 7.0, 50 mM, at 25 °C).

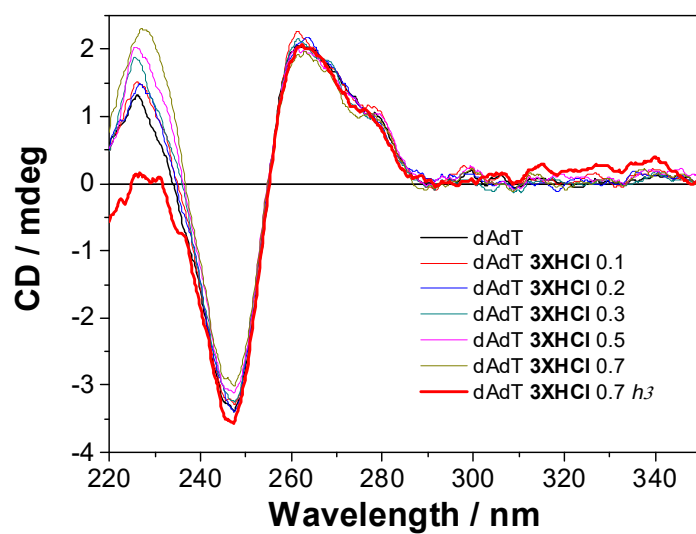


Fig. S52. CD spectra of poly dAdT – poly dAdT ($c = 2.0 \times 10^{-5}$ M) in the presence of different ratios $r[3 \times \text{HCl}]/[\text{AT-DNA}]$. The measurement was performed in cacodylate buffer / 20% DMSO (pH 7.0, 50 mM, at 25 °C).

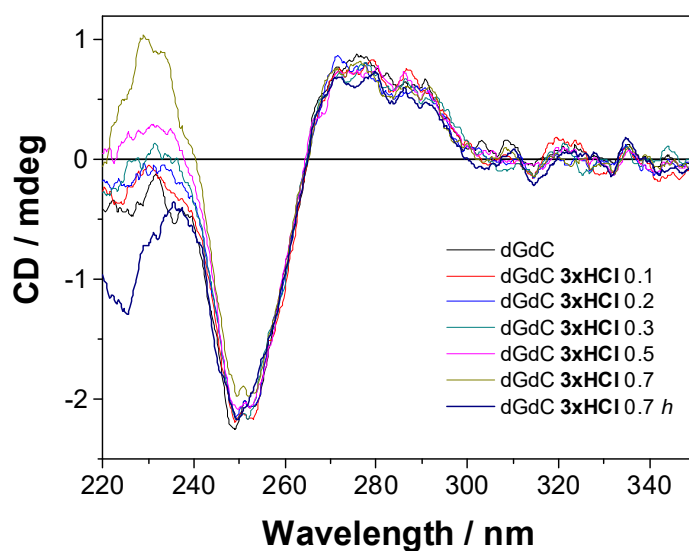


Fig. S53. CD spectra of poly dGdC – poly dGdC ($c = 2.0 \times 10^{-5}$ M) in the presence of different ratios $r[3 \times \text{HCl}]/[\text{GC-DNA}]$. The measurement was performed in cacodylate buffer (pH 7.0, 50 mM, at 25 °C).

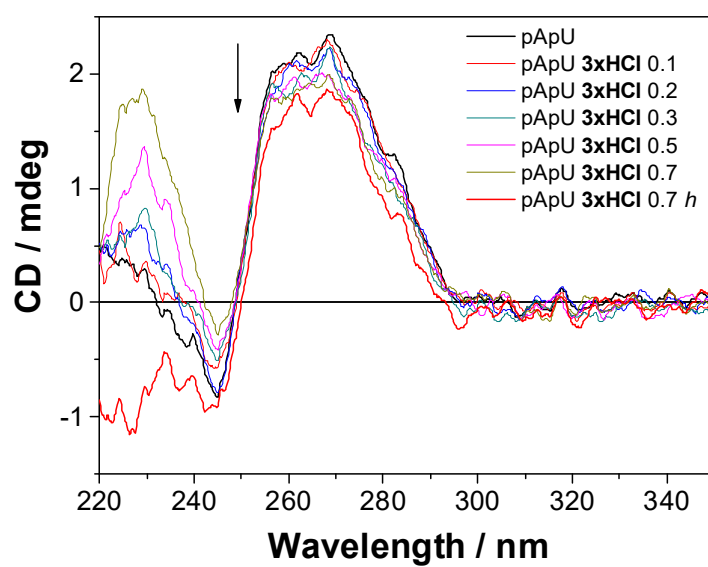


Fig. S54. CD spectra of poly A – poly U ($c = 2.0 \times 10^{-5}$ M) in the presence of different ratios $r[3 \times \text{HCl}]/[\text{AU-RNA}]$. The measurement was performed in cacodylate buffer (pH 7.0, 50 mM, at 25 °C).

5. Covalent binding to oligonucleotides

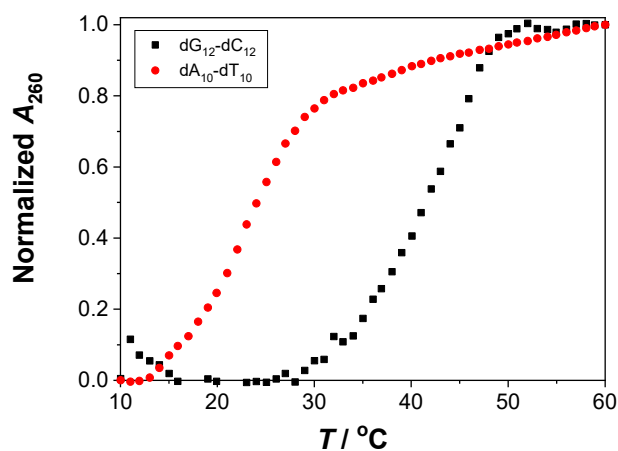


Fig. S55. Thermal denaturation of $\text{dG}_{12}\text{-dC}_{12}$ and $\text{dA}_{10}\text{-dT}_{10}$ ($c = 2.0 \times 10^{-5} \text{ M}$) in ammonium acetate buffer (pH = 7.0, 100 mM). The measured T_m for $\text{dG}_{12}\text{-dC}_{12}$ is 40 °C, and for $\text{dA}_{10}\text{-dT}_{10}$ is 22 °C.

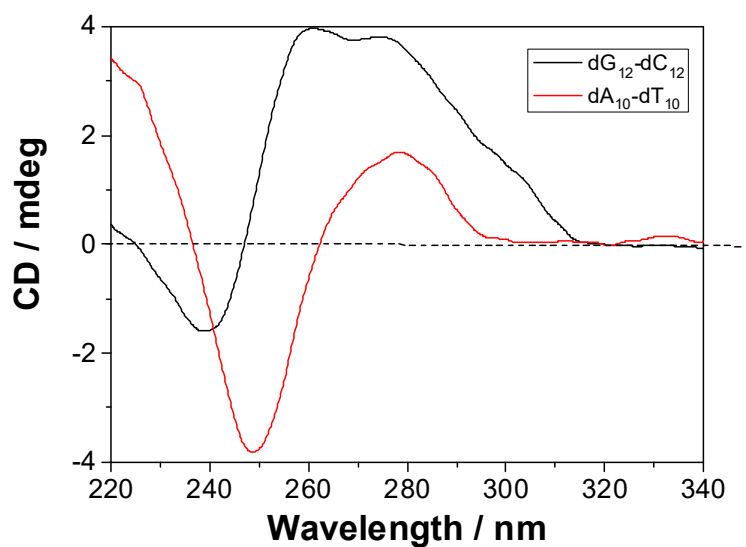


Fig. S56. CD spectra of $\text{dG}_{12}\text{-dC}_{12}$ and $\text{dA}_{10}\text{-dT}_{10}$ ($c = 2.0 \times 10^{-5} \text{ M}$) in ammonium acetate buffer (pH = 7.0, 100 mM) at 25 °C.

Analyses of the solutions containing annealed oligonucleotides and **3×HCl** were performed on a Shimadzu HPLC equipped with a dyode array detector and a PLRP-S 5 µm column. The parameters for the chromatography method are given in Table S4.

Table S4. Chromatography method for the analysis of oligonucleotides and **3×HCl**.

<i>t</i> / min	B (%)
0	5
5	5
15	40
20	100
25	100
32	5
40	5

A: NH₄Ac (100 mM, pH 7.0)

B: ACN

Flow rate: 0.5 mL/ min.

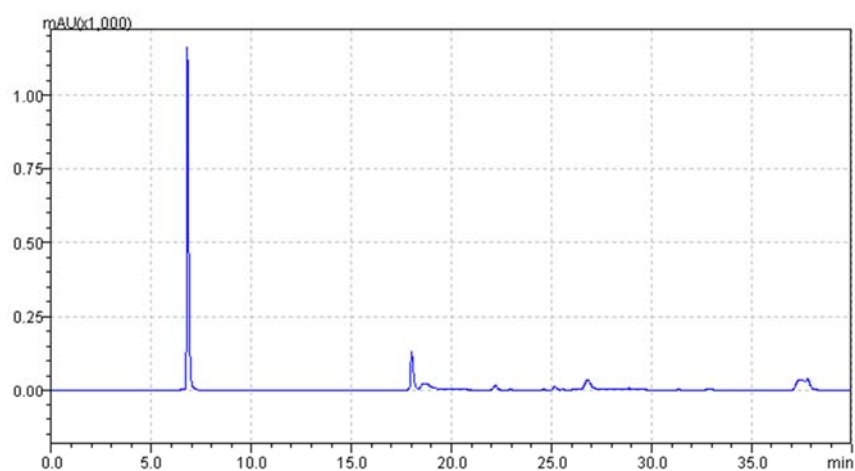


Fig. S57. HPLC chromatogram of dG₁₂-dC₁₂.

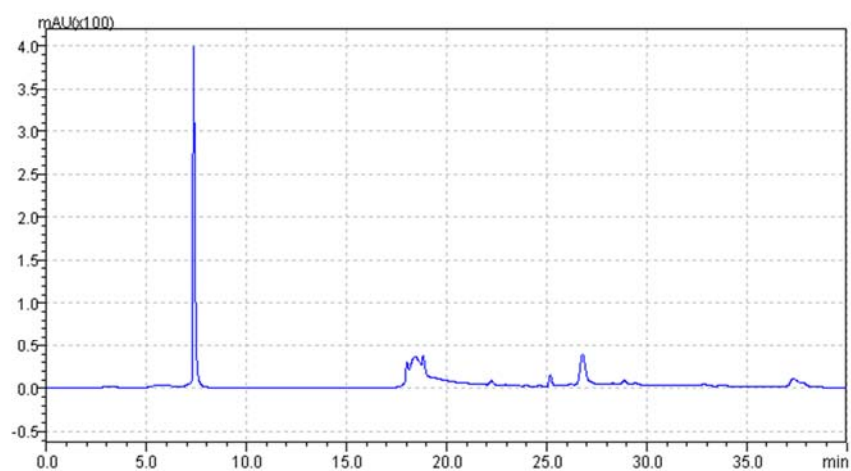


Fig. S58. HPLC chromatogram of dG₁₂-dC₁₂ after 15 min irradiation at 300 nm (8 lamps).

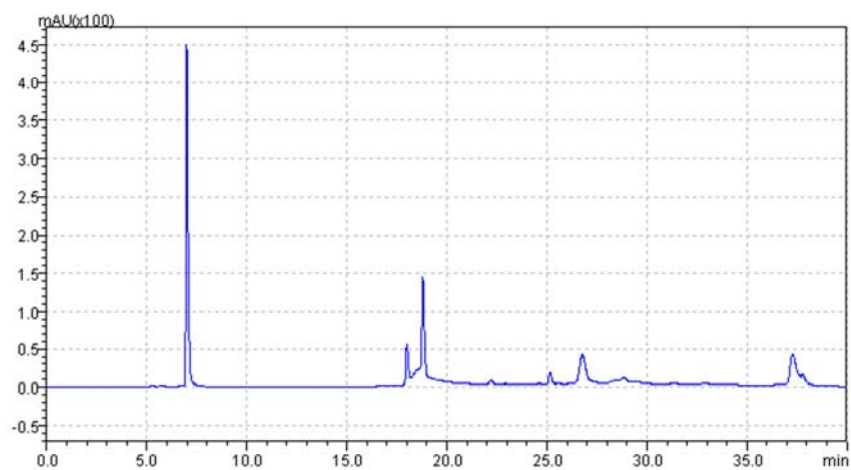


Fig. S59. HPLC chromatogram of dG₁₂-dC₁₂ and **3**×HCl before the irradiation.

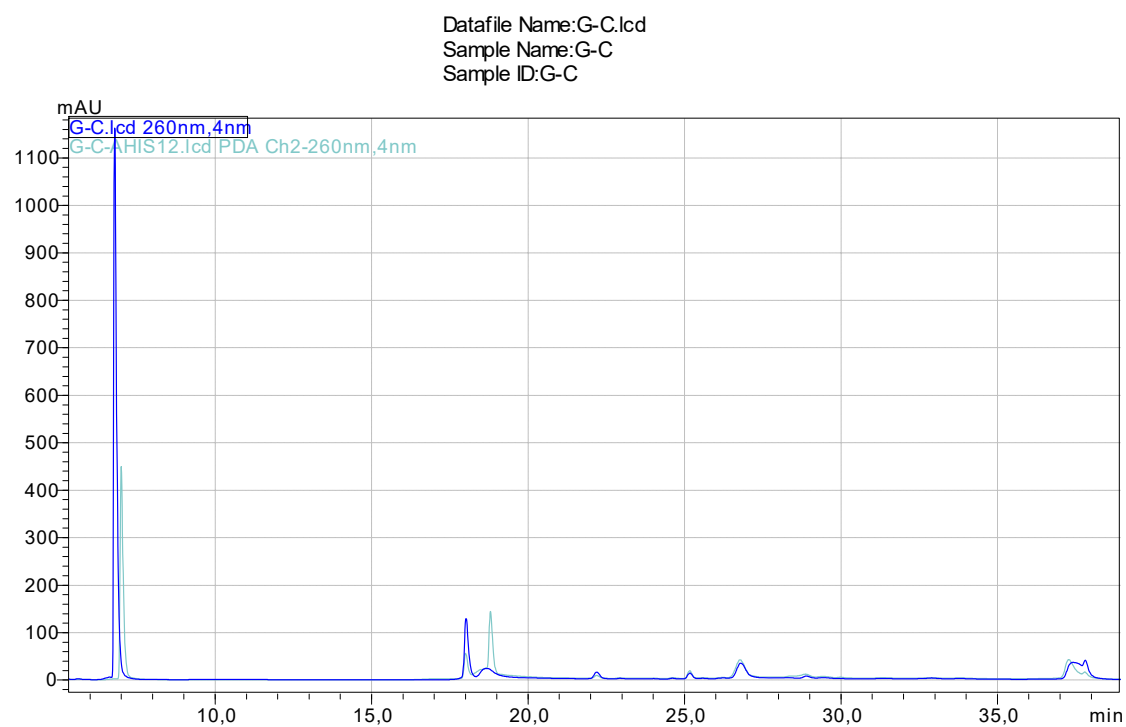


Fig. S60. Overlapped HPLC chromatogram of dG₁₂-dC₁₂ and **3**×HCl before the irradiation.

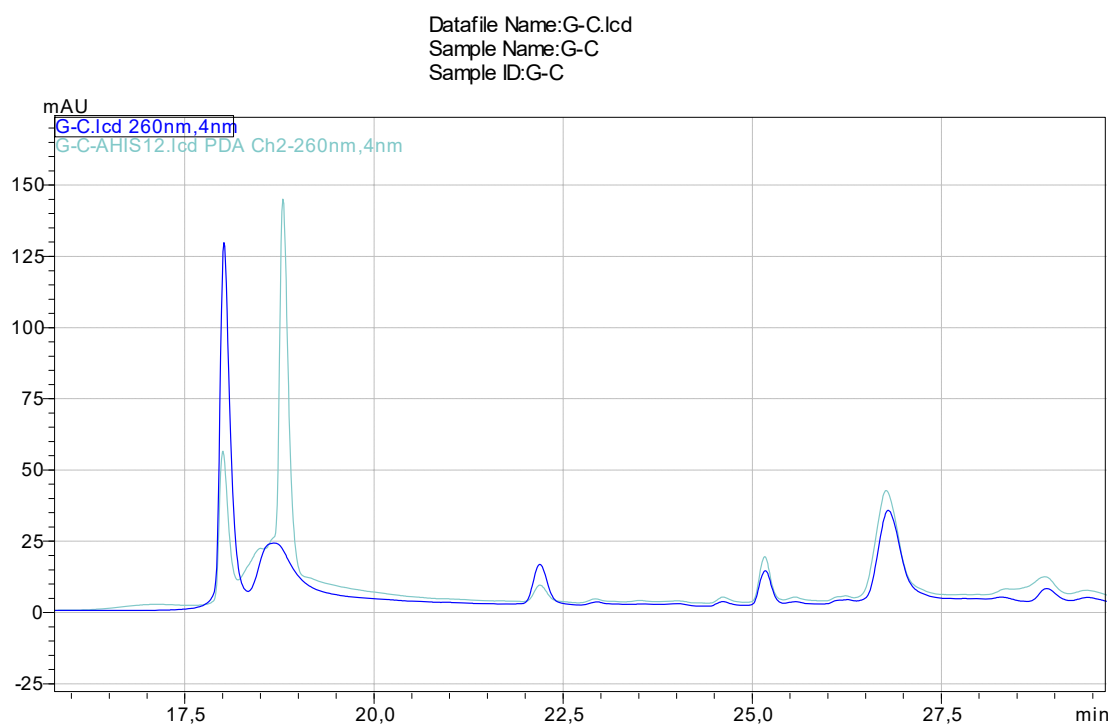


Fig. S61. Overlapped parts of HPLC chromatogram of dG₁₂-dC₁₂ and **3**×HCl before the irradiation.

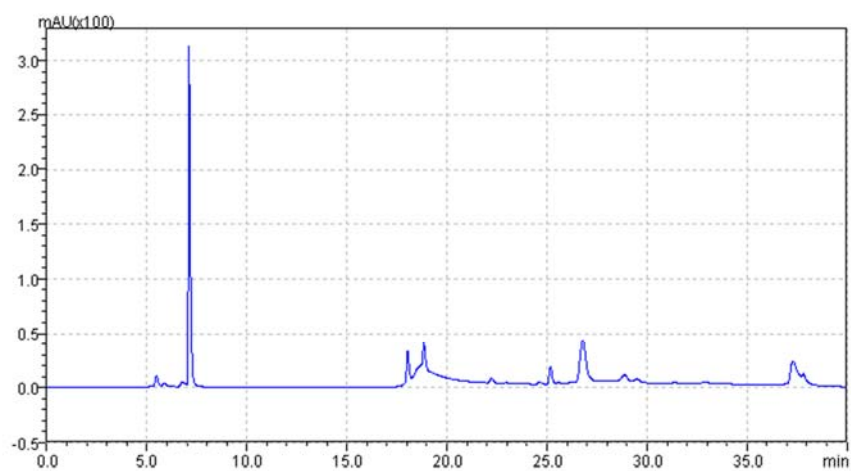


Fig. S62. HPLC chromatogram of dG₁₂-dC₁₂ and 3×HCl after 1 h irradiation at 300 nm (8 lamps).

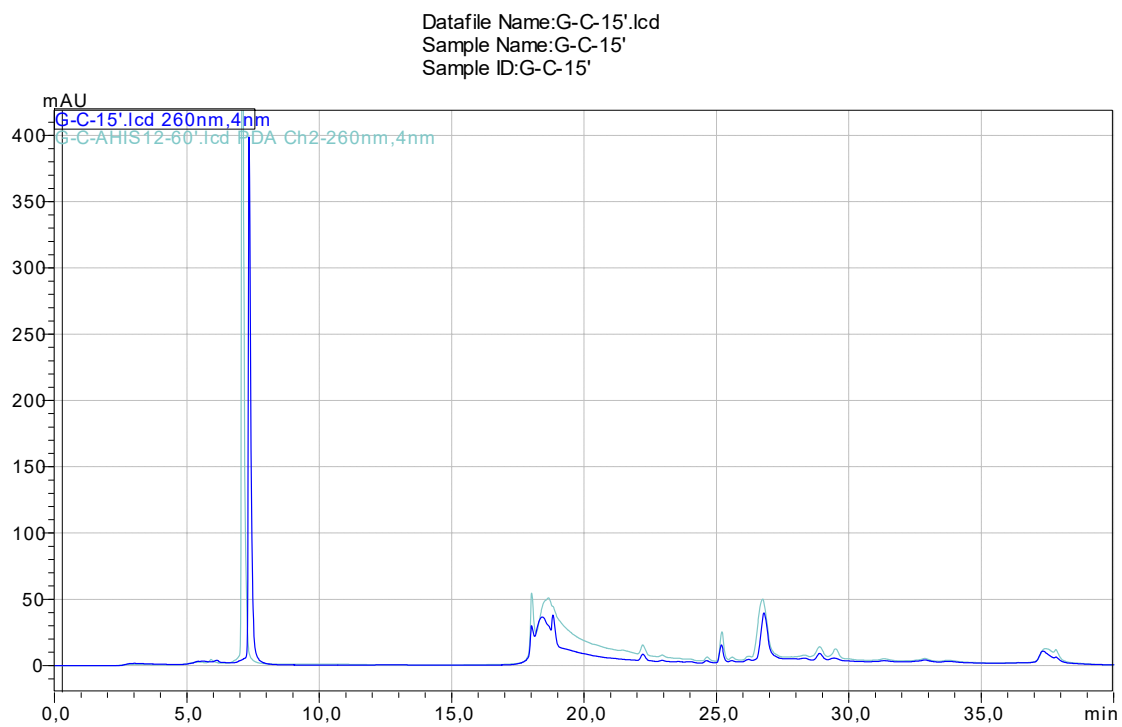


Fig. S63. Overlapped HPLC chromatogram of dG₁₂-dC₁₂ and 3×HCl after 1 h irradiation at 300 nm (8 lamps).

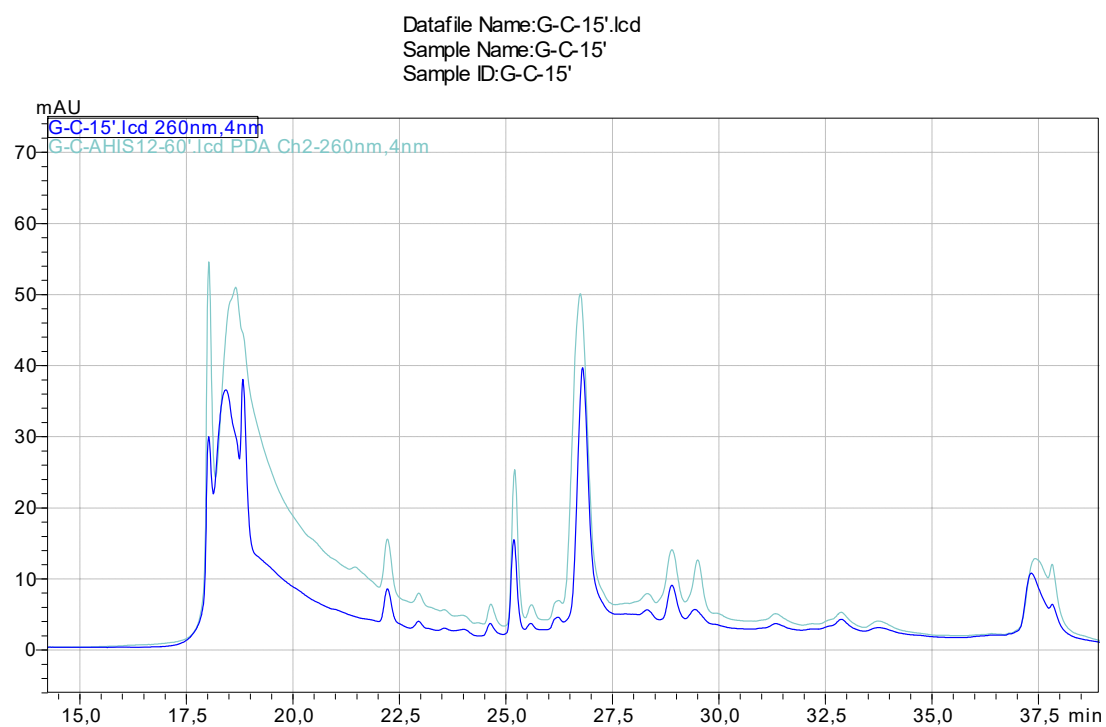


Fig. S64. Overlapped parts of HPLC chromatogram of dG₁₂-dC₁₂ and **3**×HCl after 1 h irradiation at 300 nm (8 lamps).

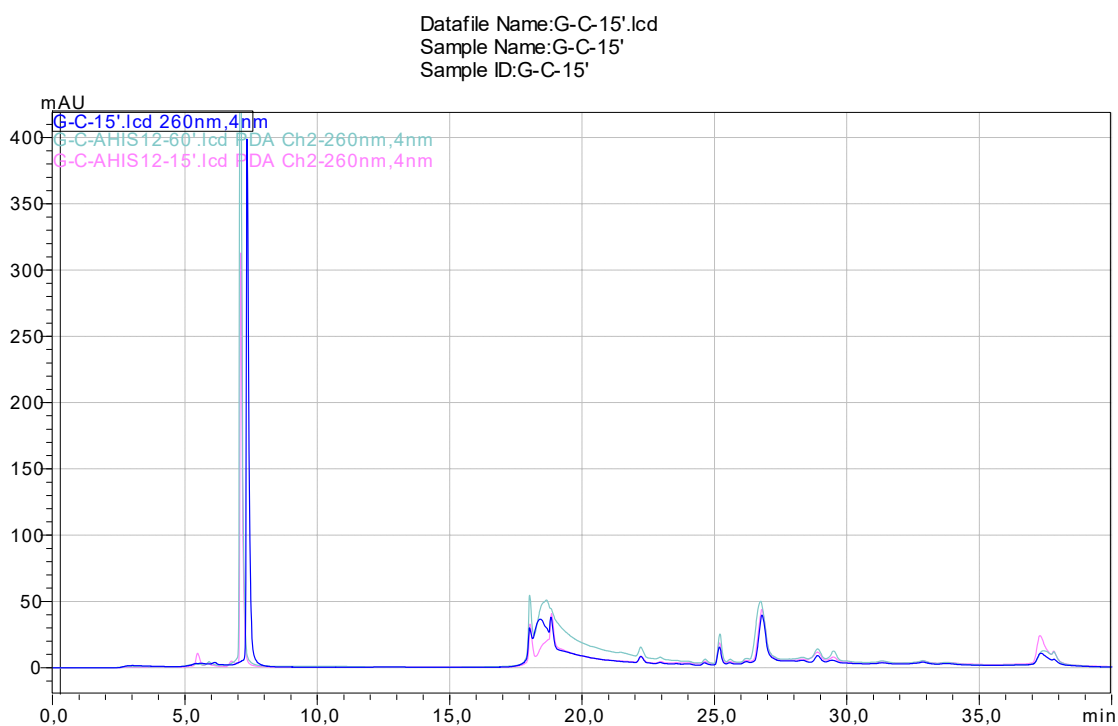


Fig. S65. Overlapped HPLC chromatogram of dG₁₂-dC₁₂ and **3**×HCl after 1 h irradiation at 300 nm (8 lamps).

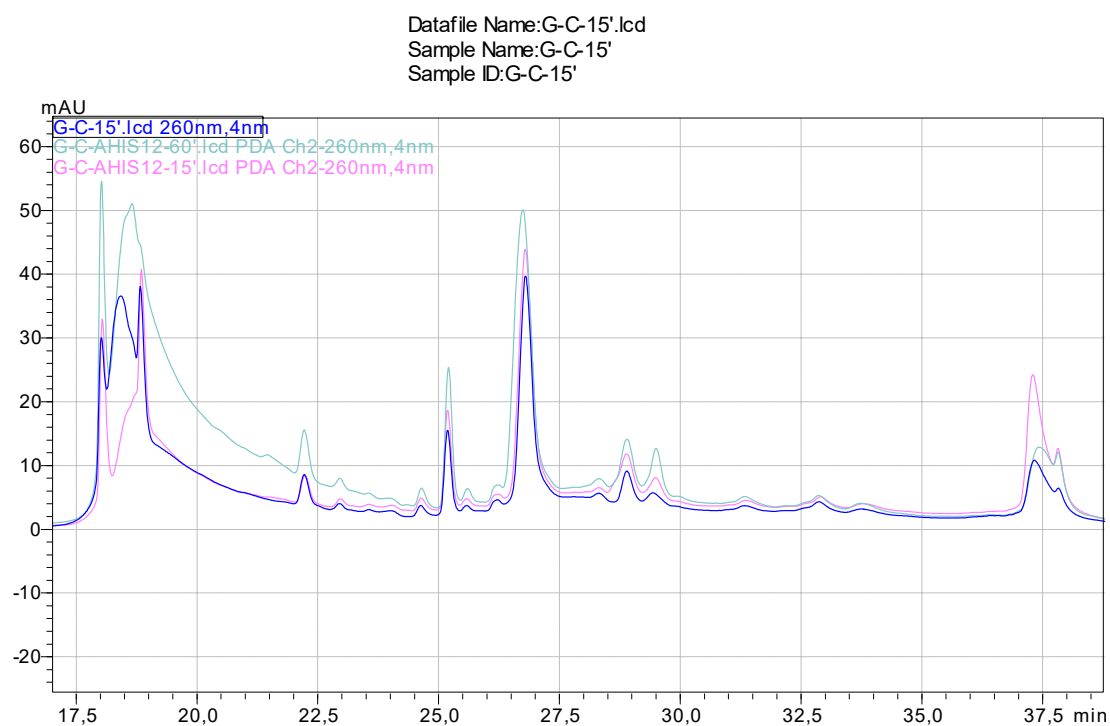


Fig. S66. Overlapped parts of HPLC chromatogram of dG₁₂-dC₁₂ and **3**×HCl after 1 h irradiation at 300 nm (8 lamps).

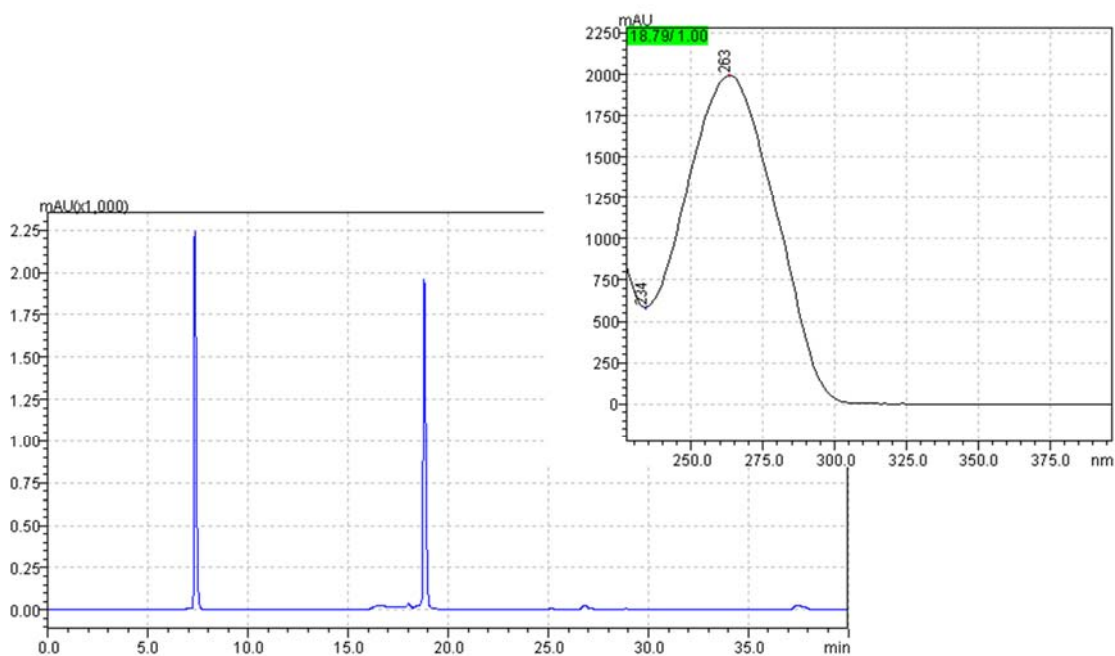


Fig. S67. HPLC chromatogram of dA₁₀-dT₁₀ (inset: absorption spectrum of the species with rt 18.8 min).

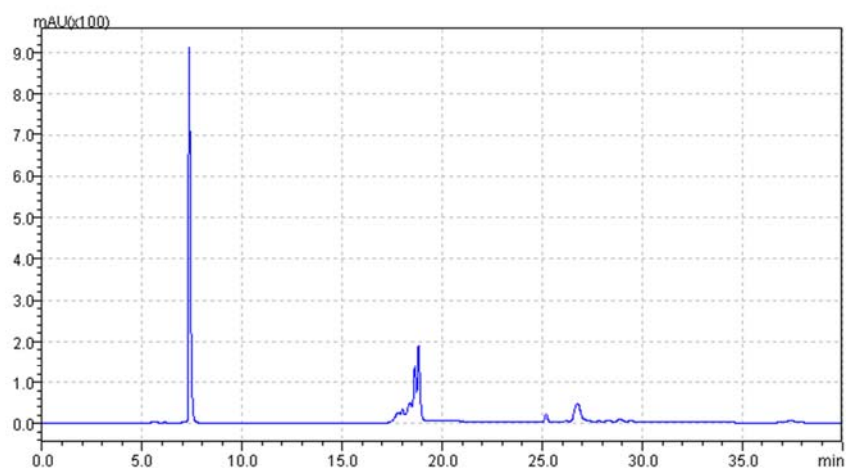


Fig. S68. HPLC chromatogram of dA₁₀-dT₁₀ after 15 min irradiation at 300 nm (8 lamps).

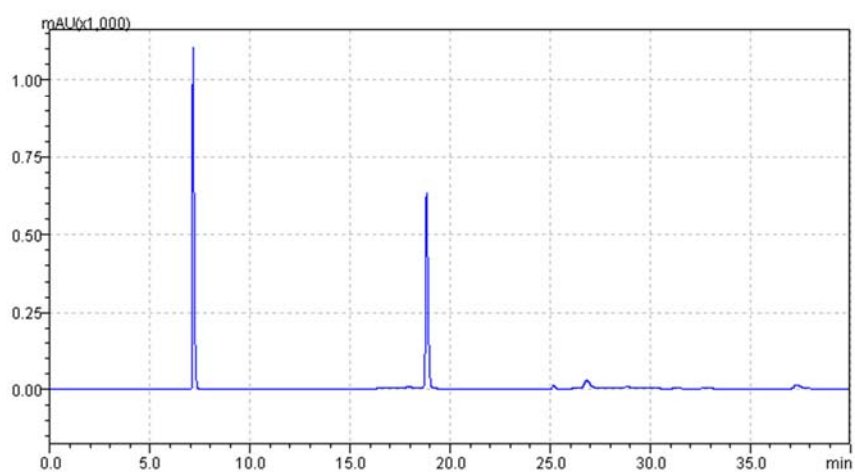


Fig. S69. HPLC chromatogram of dA₁₀-dT₁₀ and 3×HCl before the irradiation.

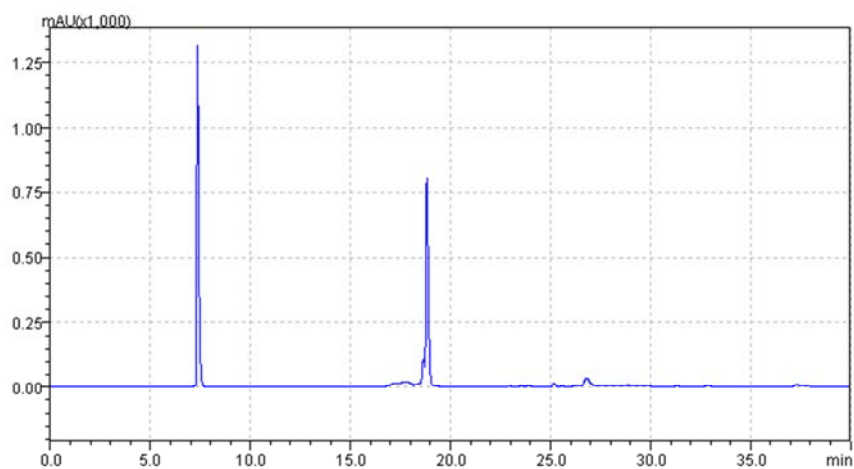


Fig. S70. HPLC chromatogram of dA₁₀-dT₁₀ and **3**×HCl after 1 h irradiation at 300 nm (8 lamps).

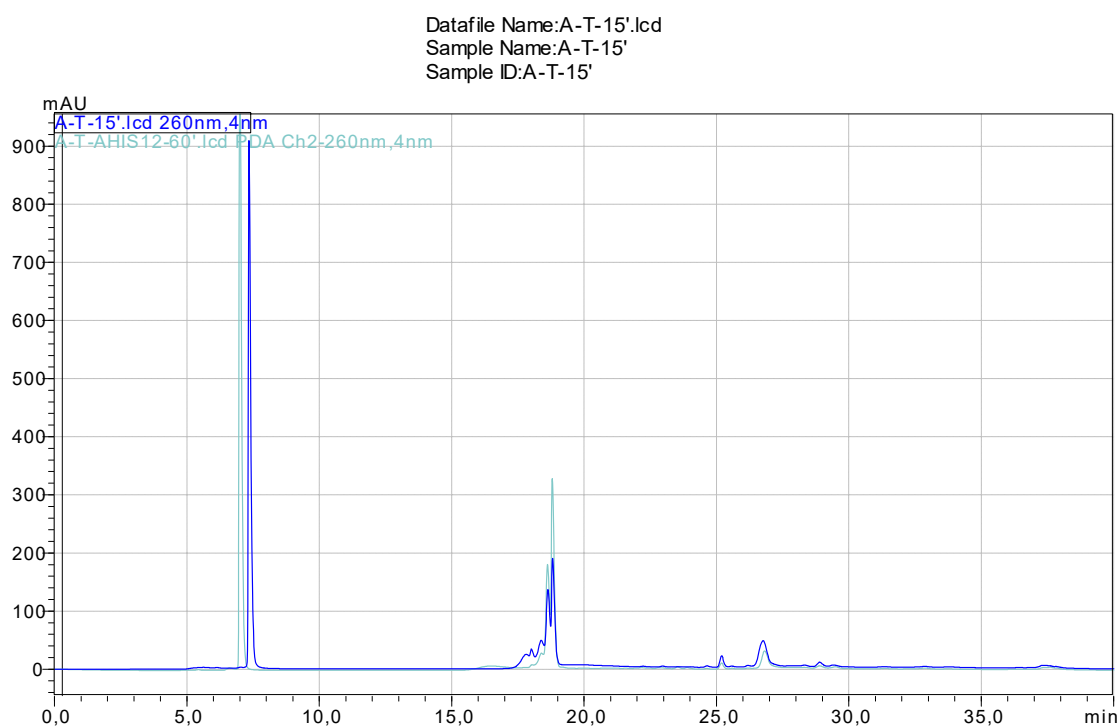


Fig. S71. Overlapped HPLC chromatogram of dA₁₀-dT₁₀ and **3**×HCl after 1 h irradiation at 300 nm (8 lamps).

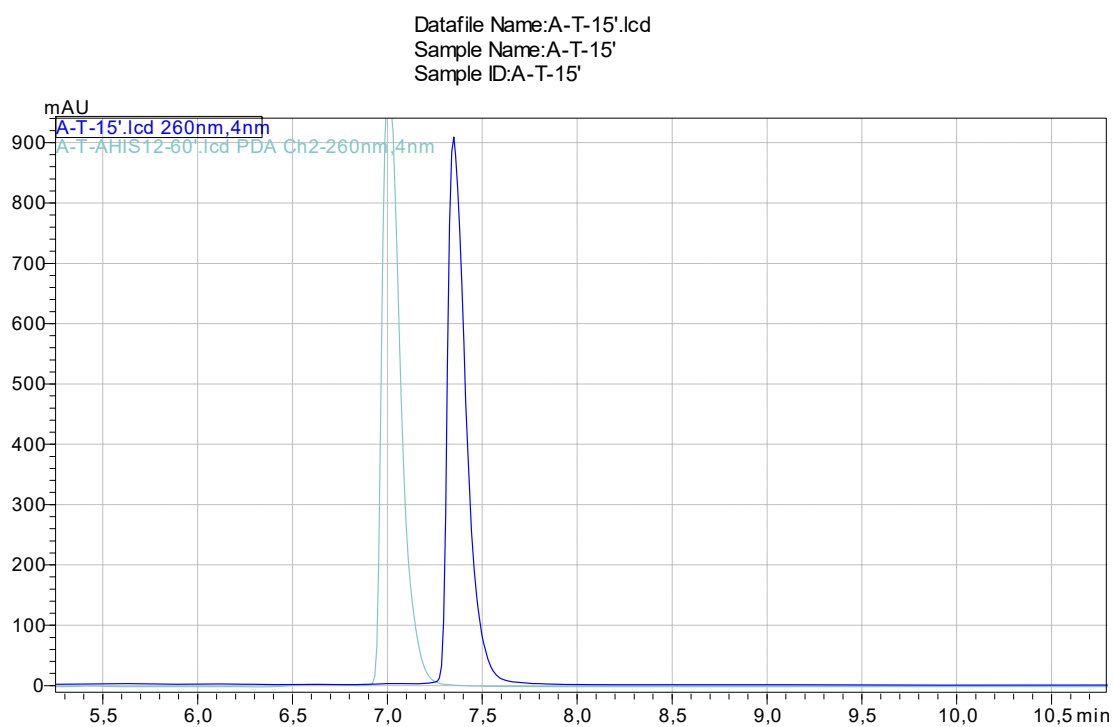


Fig. S72. Overlapped parts of HPLC chromatogram of dA₁₀-dT₁₀ and 3×HCl after 1 h irradiation at 300 nm (8 lamps).

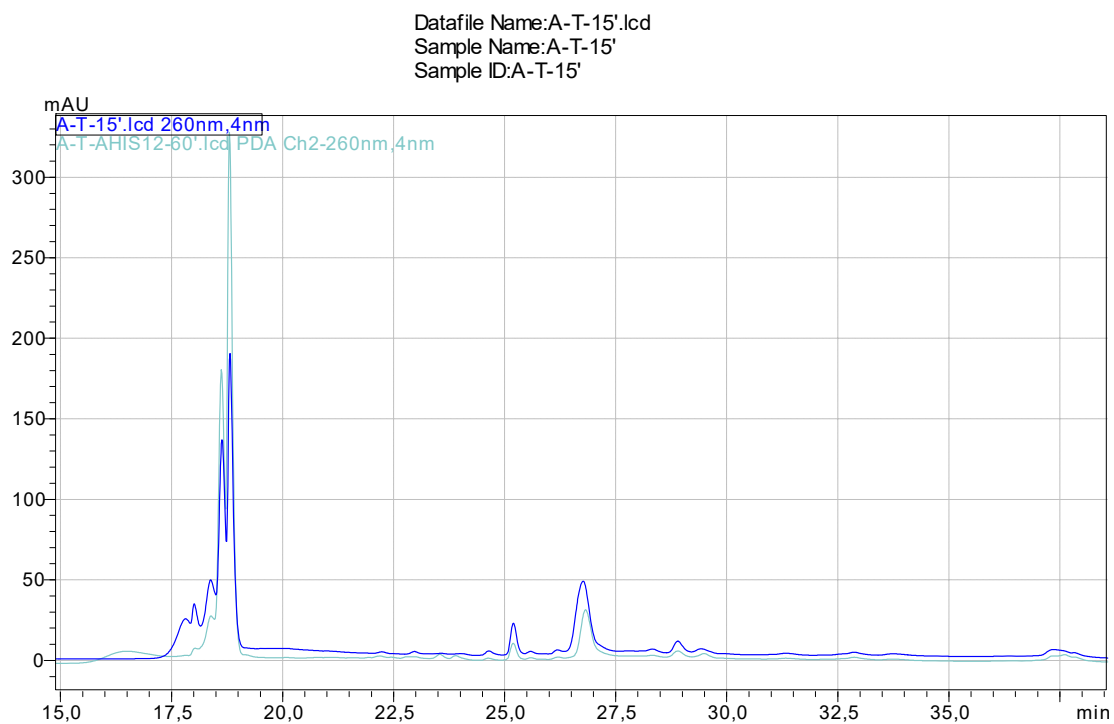


Fig. S73. Overlapped parts of HPLC chromatogram of dA₁₀-dT₁₀ and 3×HCl after 1 h irradiation at 300 nm (8 lamps).

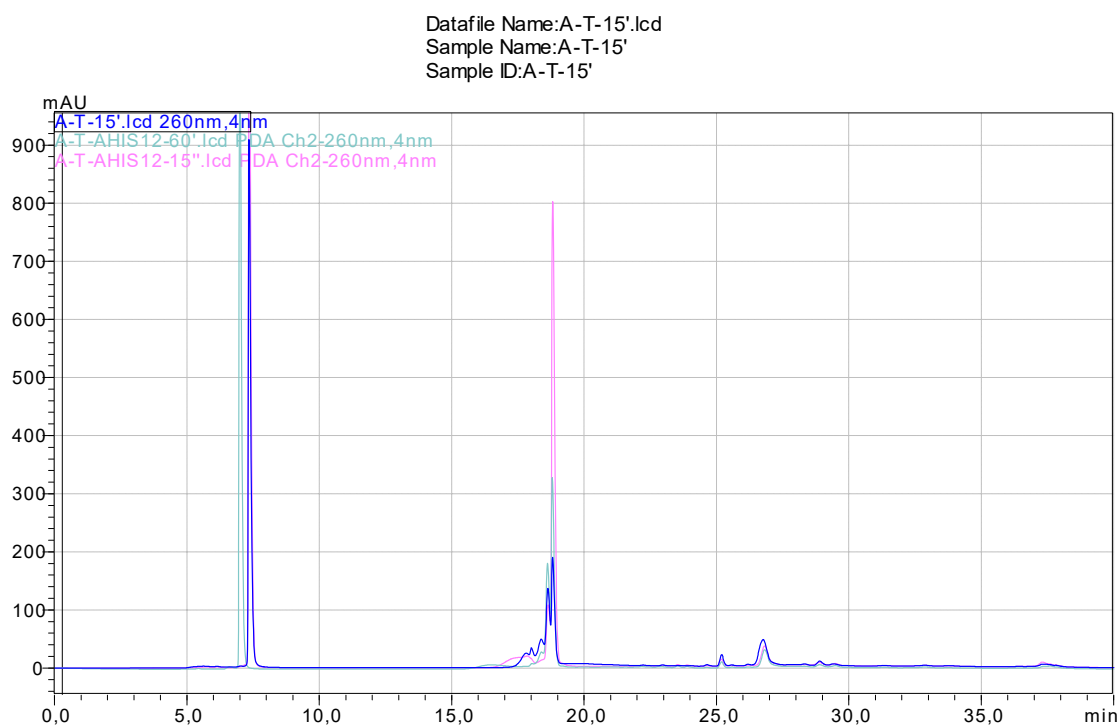


Fig. S74. Overlapped HPLC chromatogram of dA₁₀-dT₁₀ and 3×HCl after 15 min and 1 h irradiation at 300 nm (8 lamps).

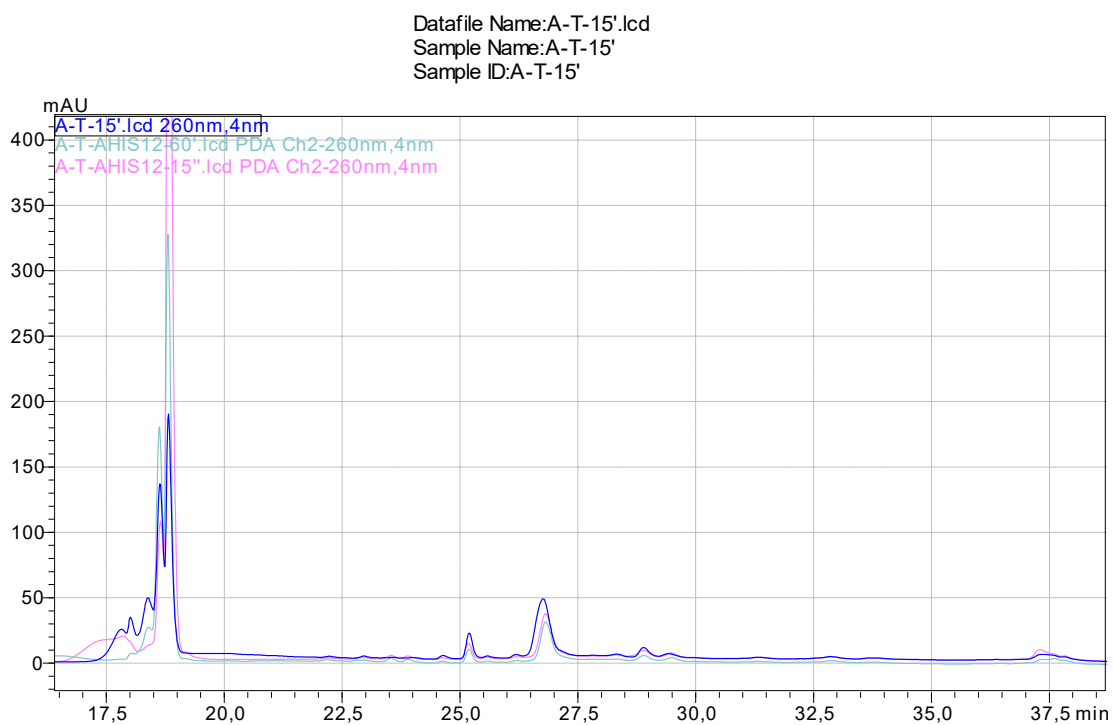
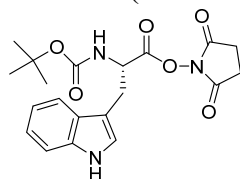


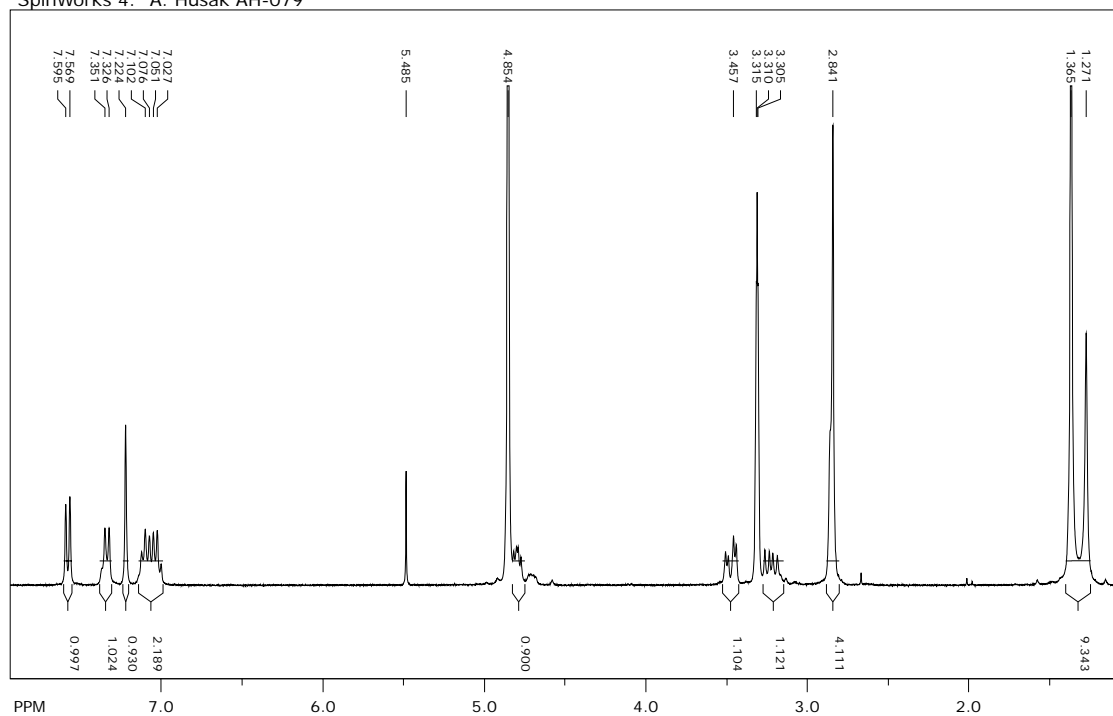
Fig. S75. Overlapped parts of HPLC chromatogram of dA₁₀-dT₁₀ and 3×HCl after 15 min and 1 h irradiation at 300 nm (8 lamps).

5. NMR spectra

^1H NMR (CD_3OD , 300 MHz) of *N*-Boc-L-Trp-OSu



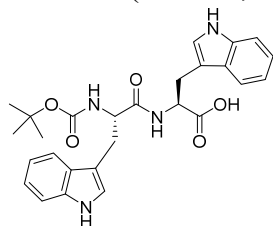
SpinWorks 4: A. Husak AH-079



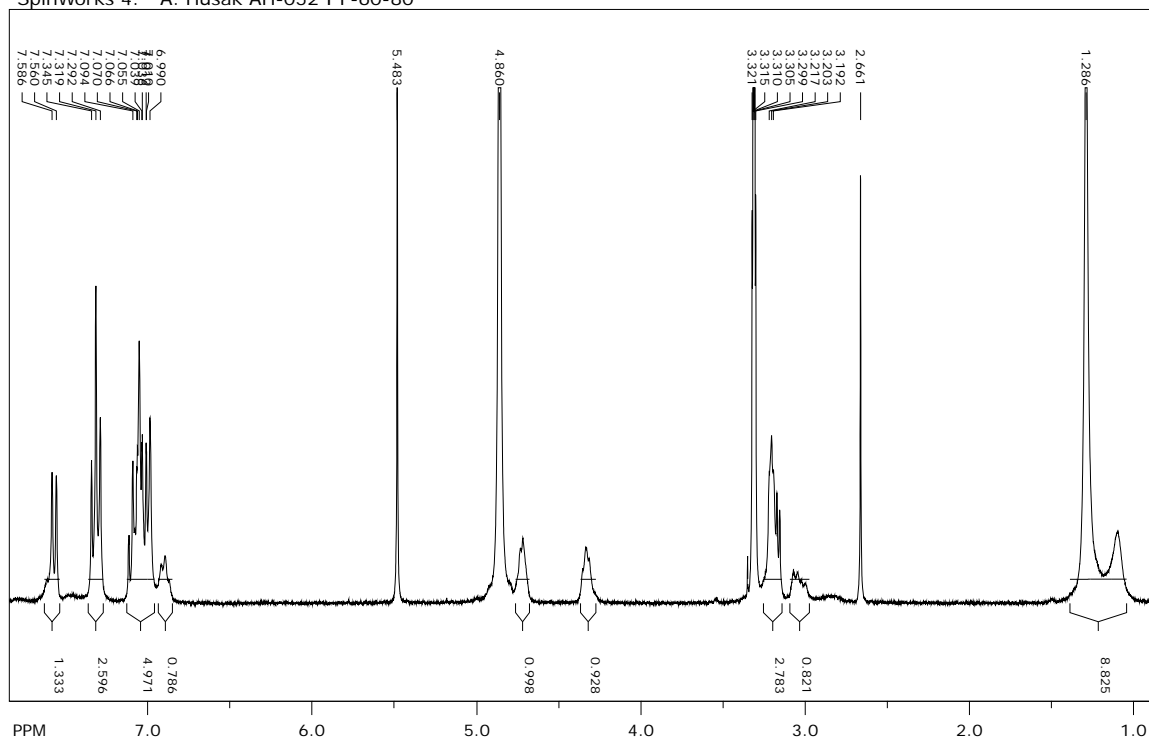
file: ...ktri\Spekttri-ESFVAH079\spectrum.dx expt: <zg30>
transmitter freq.: 300.132701 MHz
time domain size: 32768 points
width: 6172.84 Hz = 20.5670 ppm = 0.188380 Hz/pt
number of scans: 0

freq. of 0 ppm: 300.130005 MHz
processed size: 32768 complex points
LB: 0.000 GF: 0.0000

^1H NMR (CD_3OD , 300 MHz) of *N*-**Boc**-L-Trp-L-Trp-OH



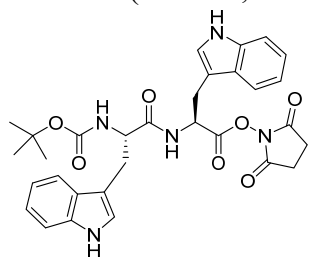
SpinWorks 4: A. Husak AH-052 I F-60-80



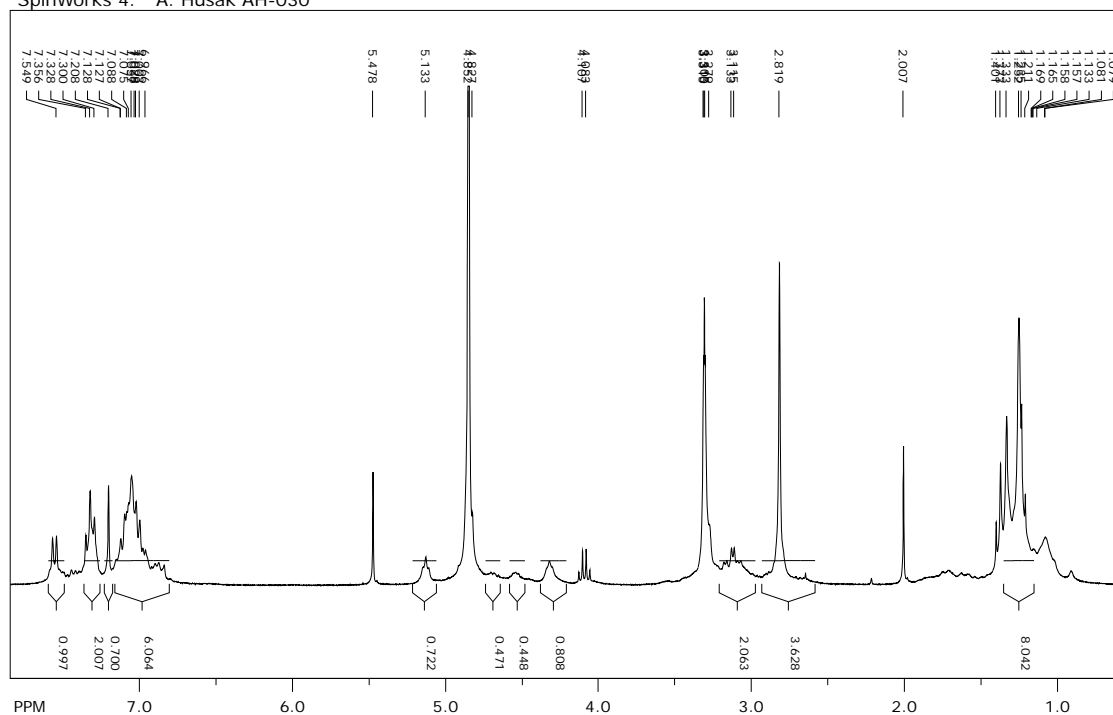
file: ...\\AH052\\AH052 I F-60-80\\spectrum.dx expt: <zg30>
 transmitter freq.: 300.132701 MHz
 time domain size: 32768 points
 width: 6172.84 Hz = 20.5670 ppm = 0.188380 Hz/pt
 number of scans: 0

freq. of 0 ppm: 300.130005 MHz
 processed size: 32768 complex points
 LB: 0.000 GF: 0.0000

¹H NMR (CD₃OD, 300 MHz) of *N*-Boc-L-Trp-L-Trp-OSu



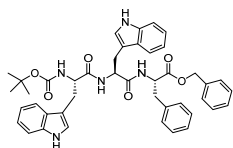
SpinWorks 4: A. Husak AH-030



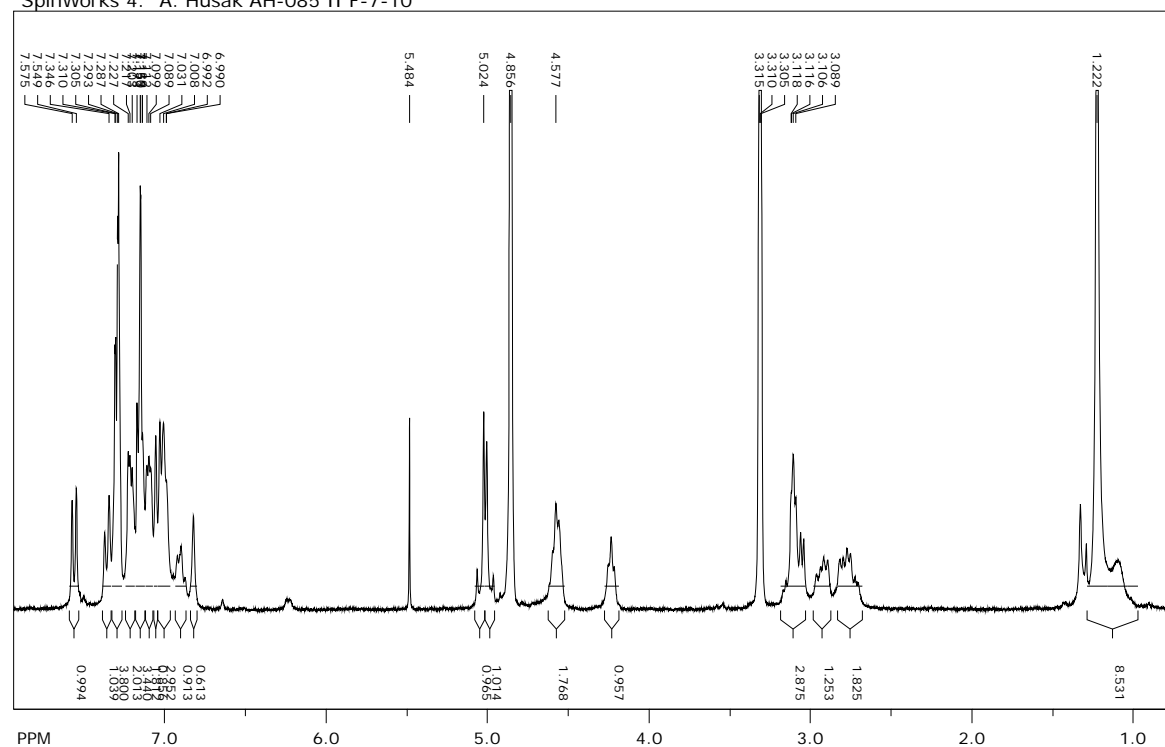
file: ...ktri\Spektri-ESF\AH030\spectrum.dx expt: <zg30>
 transmitter freq.: 300.132701 MHz
 time domain size: 32768 points
 width: 6172.84 Hz = 20.5670 ppm = 0.188380 Hz/pt
 number of scans: 0

freq. of 0 ppm: 300.130006 MHz
 processed size: 32768 complex points
 LB: 0.000 GF: 0.0000

¹H NMR (CD₃OD, 300 MHz) of **Boc-L-Trp-L-Trp-L-Phe-OBn** (**1**)



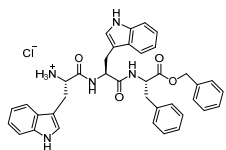
SpinWorks 4: A. Husak AH-085 II F-7-10



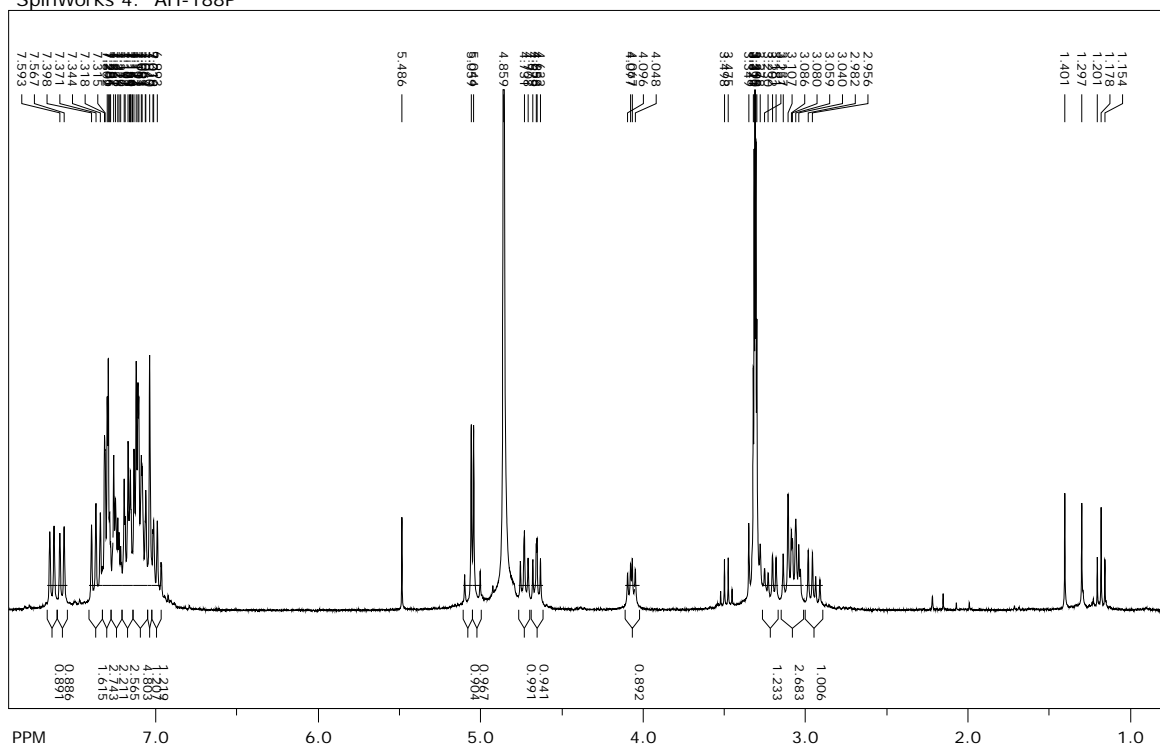
file: ...\\AH085\\AH085 II F-7-10\\spectrum.dx expt: <zg30>
 transmitter freq.: 300.132701 MHz
 time domain size: 32768 points
 width: 6172.84 Hz = 20.5670 ppm = 0.188380 Hz/pt
 number of scans: 0

freq. of 0 ppm: 300.130005 MHz
 processed size: 32768 complex points
 LB: 0.000 GF: 0.0000

^1H NMR (CD_3OD , 300 MHz) of $\text{HCl} \times \text{H-L-Trp-L-Trp-L-Phe-OBn}$ ($1 \times \text{HCl}$)



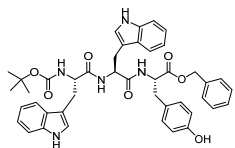
SpinWorks 4: AH-188P



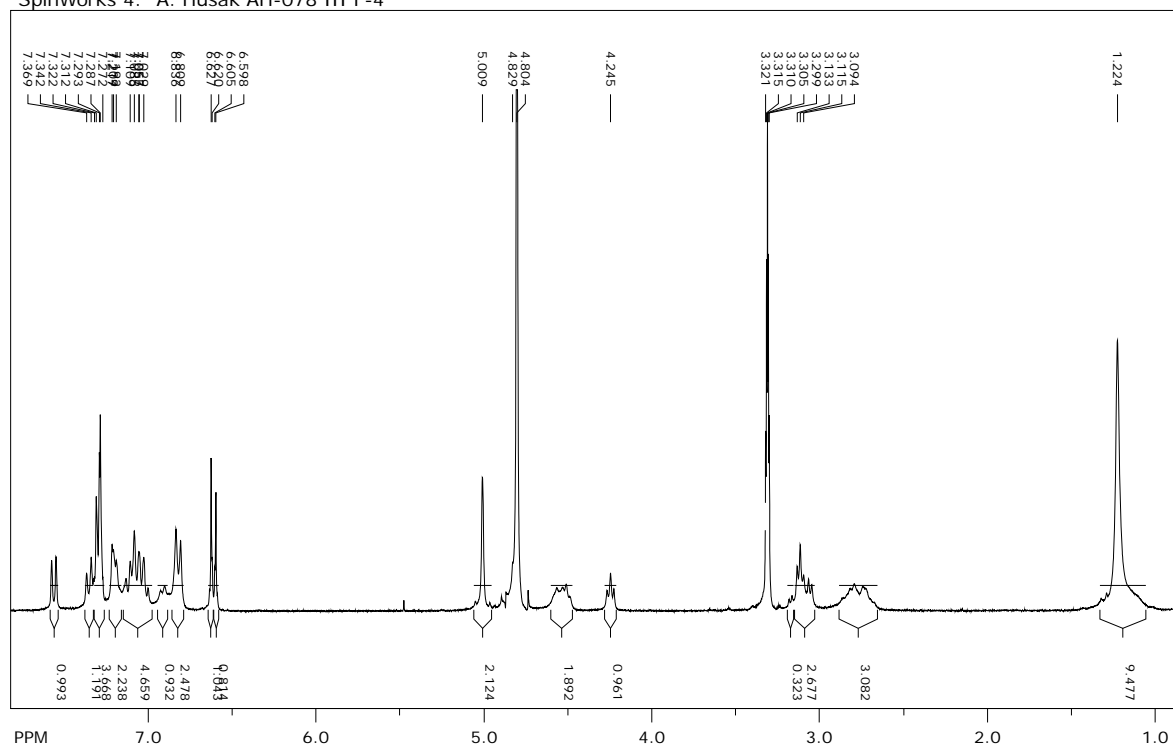
file: ...Desktop\husak_ah188p1\spectrum.dx exp: <zg30>
transmitter freq.: 300.132701 MHz
time domain size: 32768 points
width: 6172.84 Hz = 20.5670 ppm = 0.188380 Hz/pt
number of scans: 0

freq. of 0 ppm: 300.130005 MHz
processed size: 32768 complex points
LB: 0.000 GF: 0.0000

¹H NMR (CD₃OD, 300 MHz) of **Boc-L-Trp-L-Trp-L-Tyr-OBn (2)**



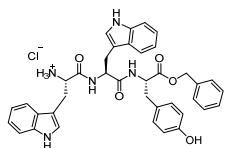
SpinWorks 4: A. Husak AH-078 III F-4



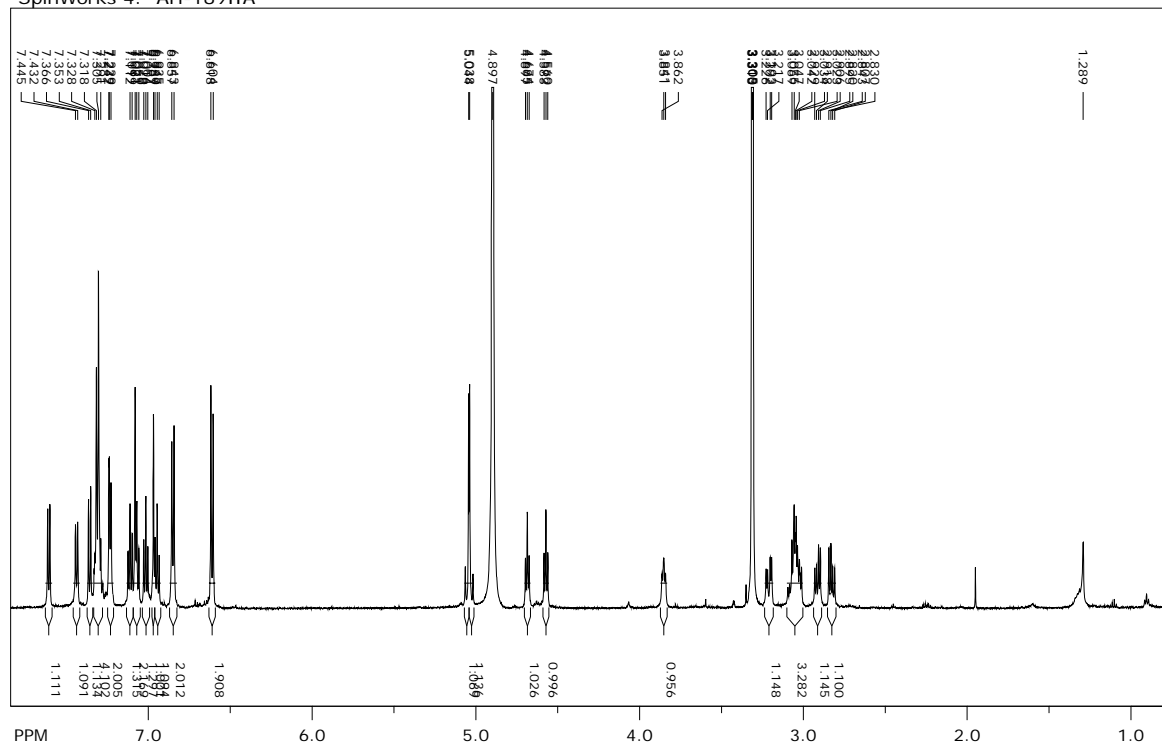
file: ...spektri\AH078 III F-4\spectrum.dx exp: <zg30>
 transmitter freq.: 300.132701 MHz
 time domain size: 32768 points
 width: 6172.84 Hz = 20.5670 ppm = 0.188380 Hz/pt
 number of scans: 0

freq. of 0 ppm: 300.130005 MHz
 processed size: 32768 complex points
 LB: 0.000 GF: 0.0000

^1H NMR (CD_3OD , 300 MHz) of $\text{HCl} \times \text{H-L-Trp-L-Trp-L-Tyr-OBn}$ ($2 \times \text{HCl}$)



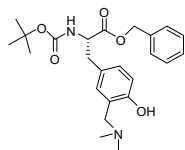
SpinWorks 4: AH-189IIA



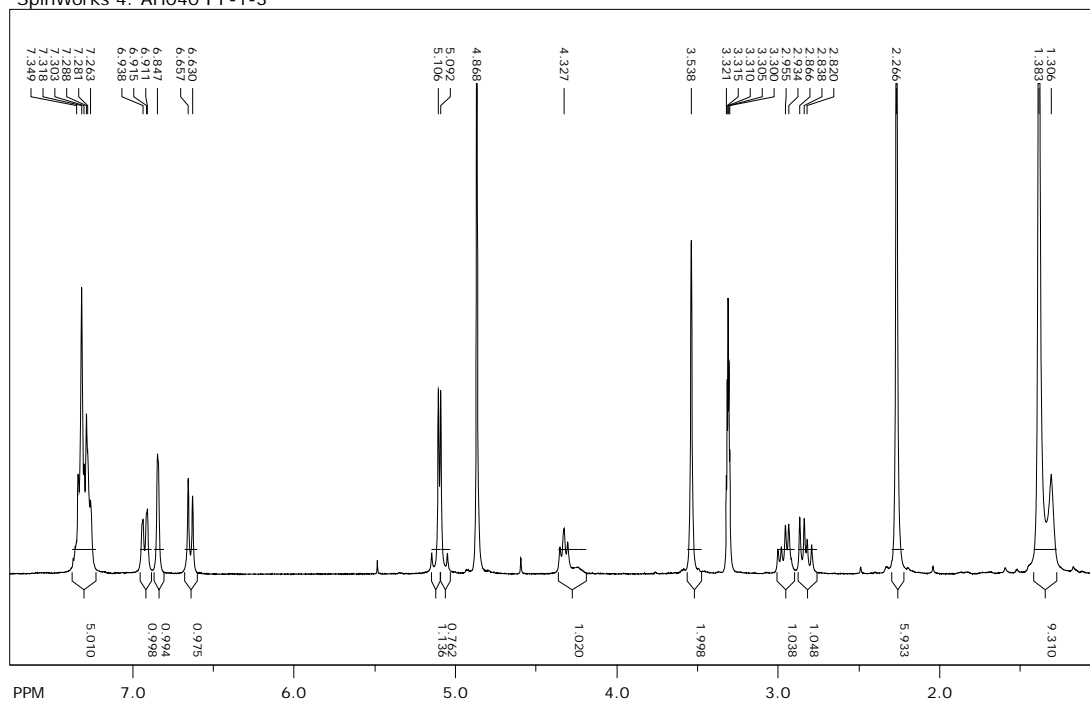
file: ...sktop\husak_ah189IIA\1\spectrum.dx expt: <zg30>
transmitter freq.: 600.135401 MHz
time domain size: 32768 points
width: 12019.23 Hz = 20.0275 ppm = 0.366798 Hz/pt
number of scans: 0

freq. of 0 ppm: 600.130007 MHz
processed size: 32768 complex points
LB: 0.000 GF: 0.0000

^1H NMR (CD_3OD , 300 MHz) of *N*-Boc-L-Tyr[$\text{CH}_2\text{N}(\text{CH}_3)_2$]-OBn



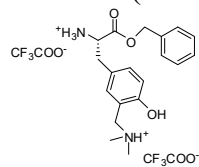
SpinWorks 4: AH040 I F-1-3



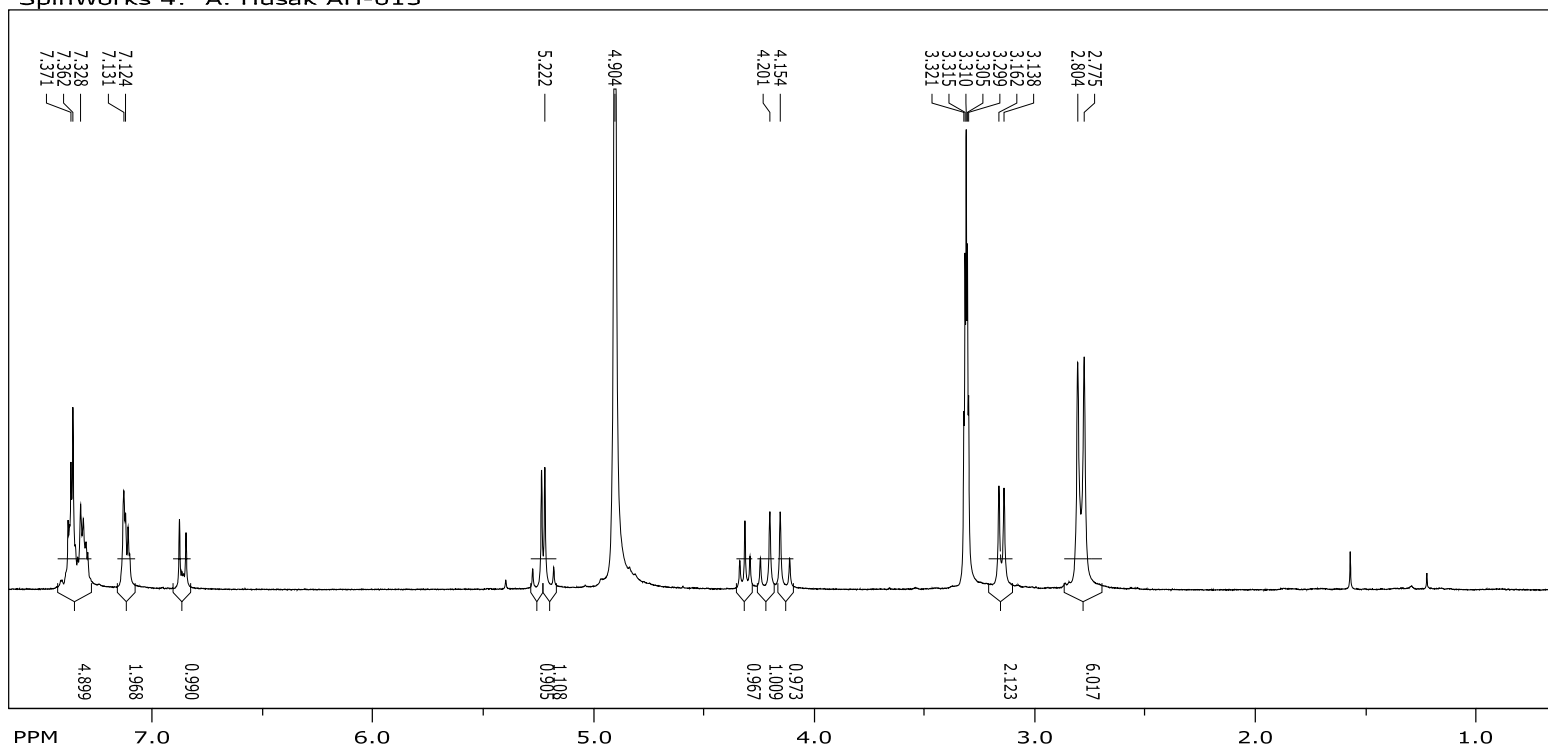
file: ...teza\BocTyr(Man)OBn\1H\spectrum.dx expt: <zg30>
 transmitter freq.: 300.132701 MHz
 time domain size: 32768 points
 width: 6172.84 Hz = 20.5670 ppm = 0.188380 Hz/pt
 number of scans: 0

freq. of 0 ppm: 300.130005 MHz
 processed size: 32768 complex points
 LB: 0.000 GF: 0.0000

^1H NMR (CD_3OD , 300 MHz) of $\text{TFA} \times \text{H-Tyr}[\text{CH}_2\text{N}(\text{CH}_3)_2 \times \text{TFA}] \cdot \text{OBn}$



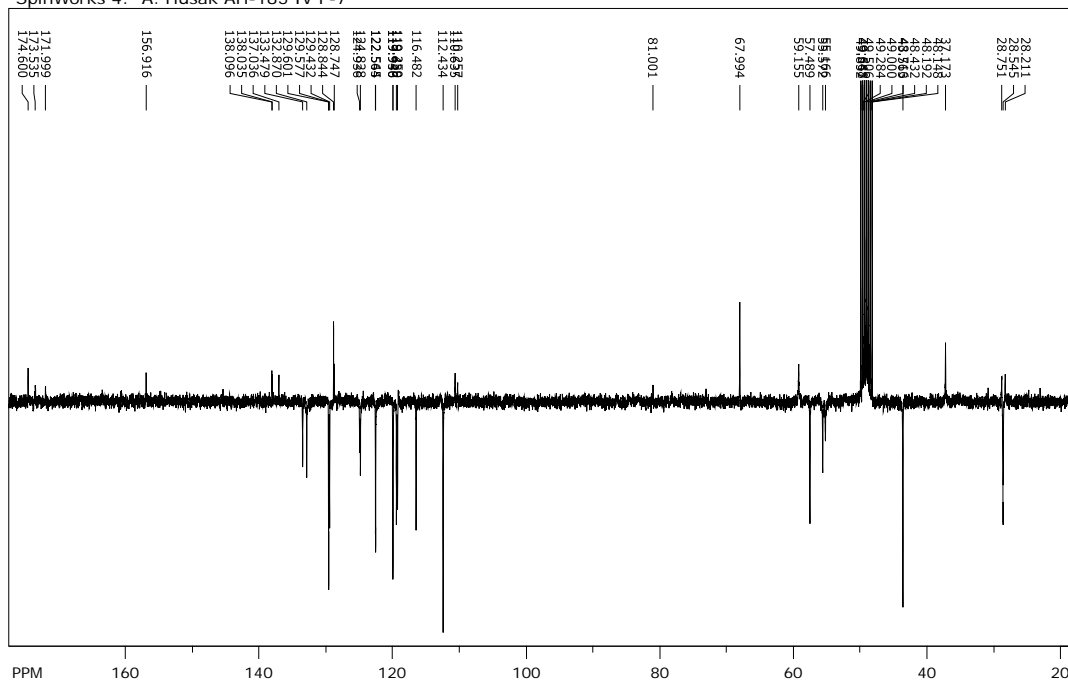
SpinWorks 4: A. Husak AH-013



file: G:\Spektri\Rad\AH013\spectrum.dx expt: <zg30>
 transmitter freq.: 300.132701 MHz
 time domain size: 32768 points
 width: 6172.84 Hz = 20.5670 ppm = 0.188380 Hz/pt
 number of scans: 0

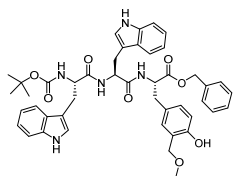
freq. of 0 ppm: 300.130005 MHz
 processed size: 32768 complex points
 LB: 0.000 GF: 0.0000



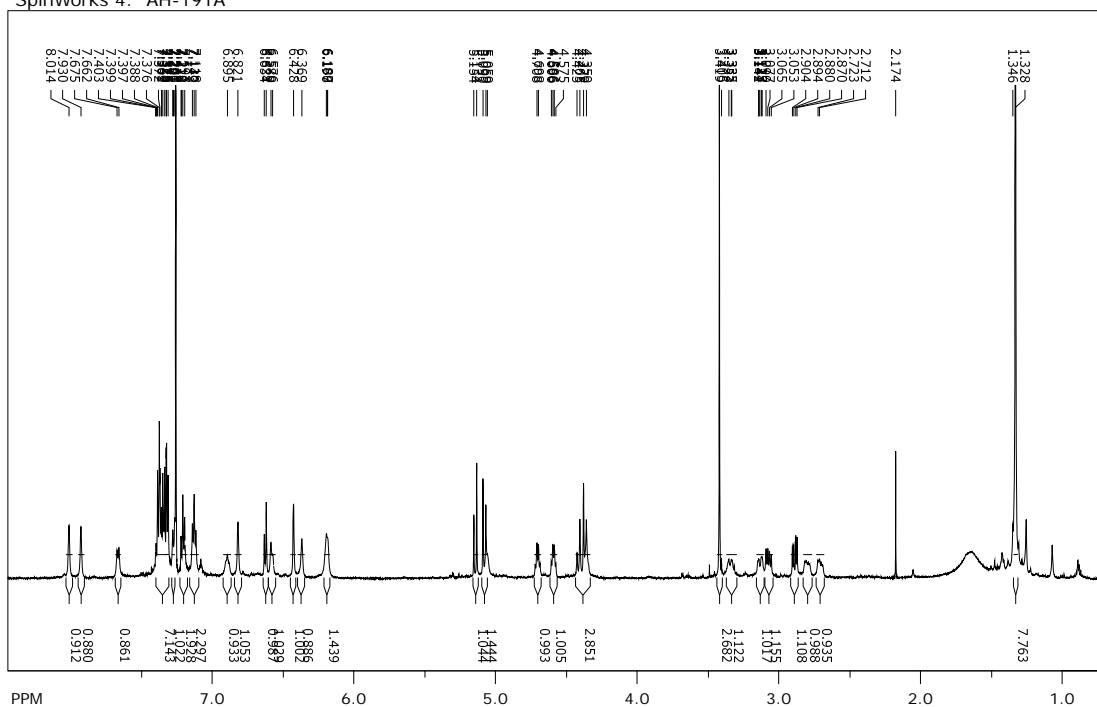
CC(C)(C)OC(=O)NC(=O)N[C@@H](Cc1c[nH]c2ccccc12)C(=O)N[C@@H](Cc1ccc(cc1)[C@H]2CN(C)CC2O)C(=O)OCc3ccccc3

freq. of 0 ppm: 75.467642 MHz
processed size: 32768 complex points
LB: 0.000 GF: 0.0000

¹H NMR (CD₃OD, 600 MHz) of *N*-Boc-L-Trp-L-Trp-L-Tyr[CH₂OCH₃]-OBn (3-OMe)

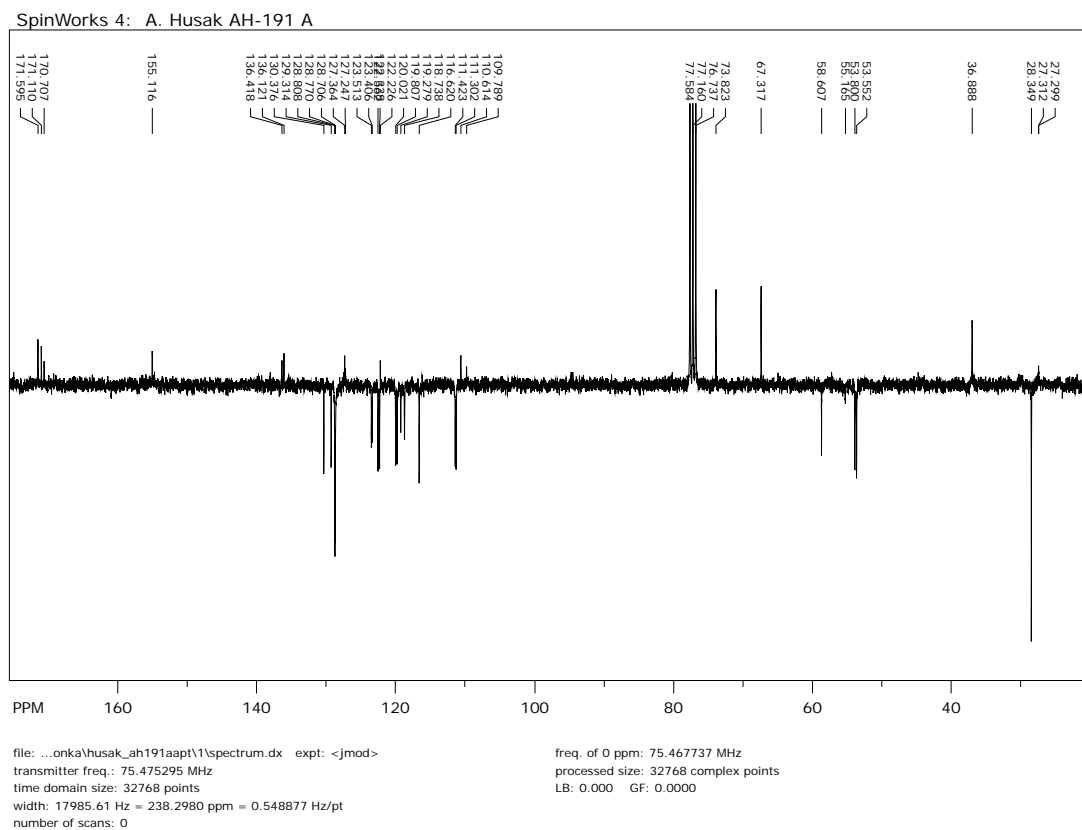
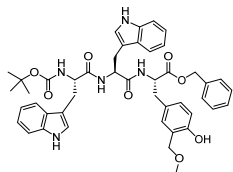


SpinWorks 4: AH-191A

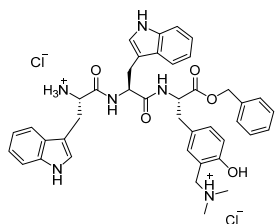


file: ...\\Spektri Tonka\\AH191 A\\spectrum.dx expt: <zg30>
 transmitter freq.: 600.135401 MHz
 time domain size: 32768 points
 width: 12019.23 Hz = 20.0275 ppm = 0.366798 Hz/pt
 number of scans: 0

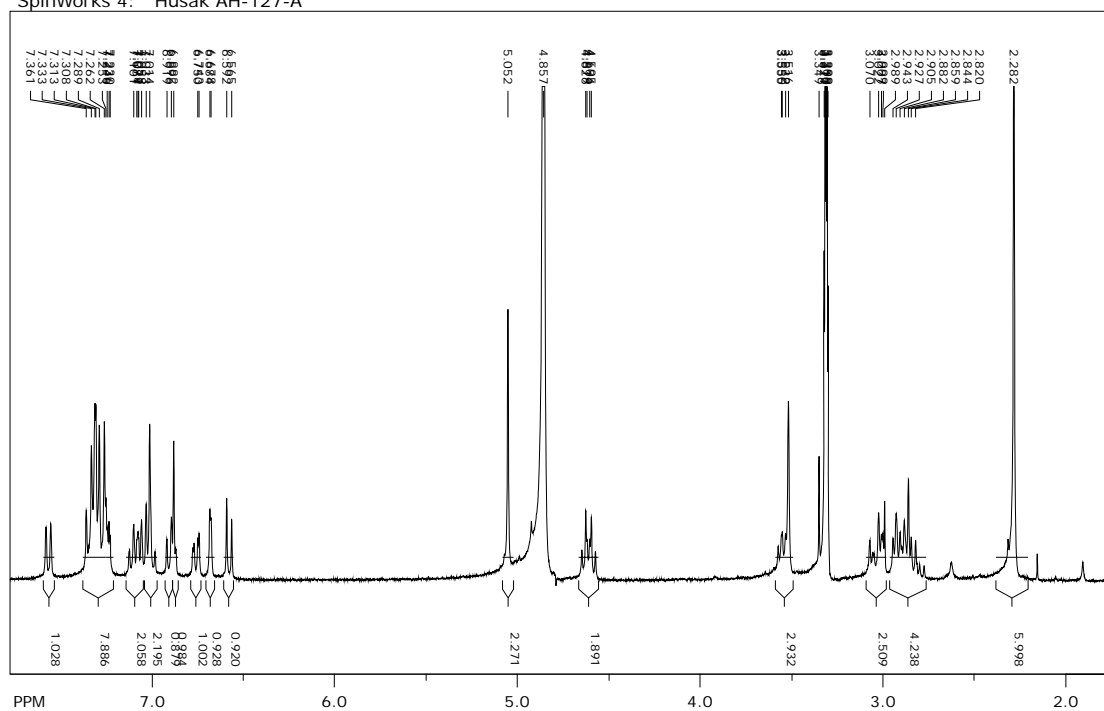
freq. of 0 ppm: 600.130010 MHz
 processed size: 32768 complex points
 LB: 0.000 GF: 0.0000

¹³C NMR (CD₃OD, 75 MHz, APT) of *N*-Boc-L-Trp-L-Trp-L-Tyr[CH₂OCH₃]-OBn (3-OMe)

^1H NMR (CD_3OD , 300 MHz) of $\text{HCl} \times \text{H-L-Trp-L-Trp-L-Tyr}[\text{CH}_2\text{N}(\text{CH}_3)_2]\text{-OBn}$ ($3 \times \text{HCl}$)



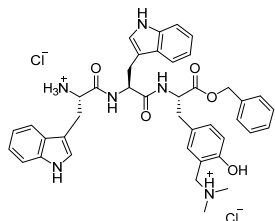
SpinWorks 4: Husak AH-127-A



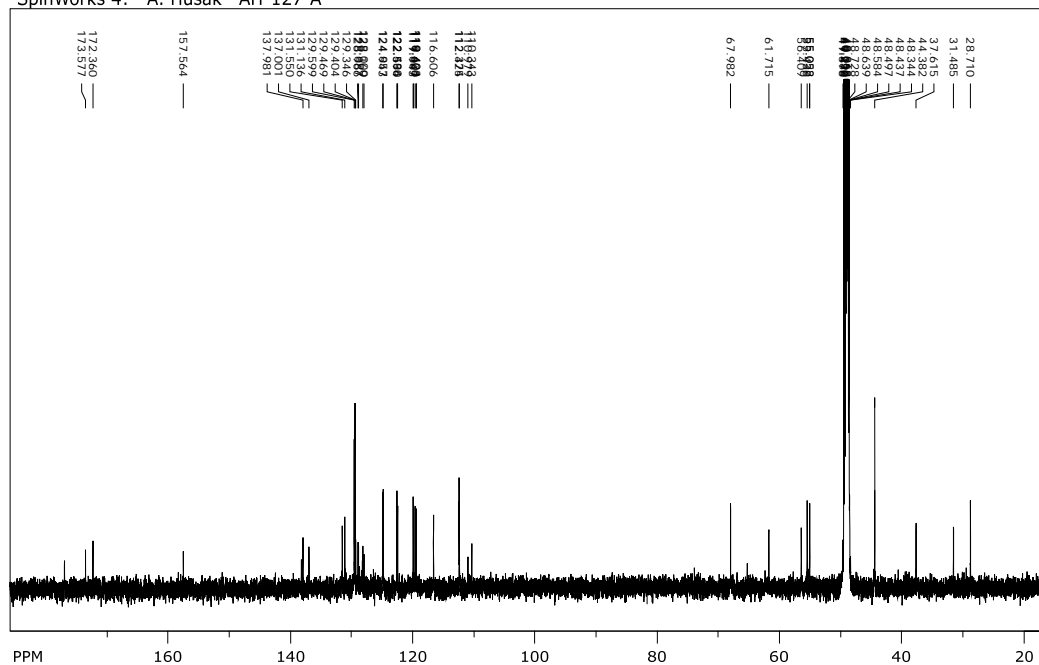
file: ...o po2ara\AH127\AH127-A\spectrum.dx exp: <zg30>
transmitter freq.: 300.132701 MHz
time domain size: 32768 points
width: 6172.84 Hz = 20.5670 ppm = 0.188380 Hz/pt
number of scans: 0

freq. of 0 ppm: 300.130005 MHz
processed size: 32768 complex points
LB: 0.000 GF: 0.0000

^{13}C NMR (CD_3OD , 150 MHz) of $\text{HCl} \times \text{H-L-Trp-L-Trp-L-Tyr}[\text{CH}_2\text{N}(\text{CH}_3)_2]\text{-OBn}$ ($3 \times \text{HCl}$)



SpinWorks 4: A. Husak AH-127-A



file: ...zara\husak_ah127ac13\2\spectrum.dx expt: <zpgp30>
transmitter freq.: 150.917899 MHz
time domain size: 32768 points
width: 35971.22 Hz = 238.3496 ppm = 1.097755 Hz/pt
number of scans: 0

freq. of 0 ppm: 150.902594 MHz
processed size: 32768 complex points
LB: 0.000 GF: 0.0000

References

- ¹ Husak, A.; Noichl, B. P.; Šumanovac Ramljak, T.; Sohora, M.; Škalamera, Đ.; Budiša, N.; Basarić, N. Photochemical Formation of Quinone Methides from Peptides Containing Modified Tyrosine. *Org. Biomol. Chem.* **2016**, *14*, 10894-10905.
- ² Kumar Mishra, N.; Ballabh Joshi, K.; Verma, S. Inhibition of Human and Bovine Insulin Fibril Formation by Designed Peptide Conjugates. *Mol. Pharmaceutics* **2013**, *10*, 3903-3912.
- ³ Chen, H.; Gao, P.; Zhang, M.; Liao, W.; Zhang, J. Synthesis and Biological Evaluation of a Novel Class of β -carboline Derivatives. *New J. Chem.* **2014**, *38*, 4155-4166.
- ⁴ Molar absorption coefficients and spectra obtained from <https://omlc.org/spectra/PhotochemCAD/html/091.html> and <https://omlc.org/spectra/PhotochemCAD/html/073.html>
- ⁵ Molar absorption coefficients and spectra obtained from <https://omlc.org/spectra/PhotochemCAD/html/092.html>.
- ⁶ Trinquet, E.; Mathis, G. Fluorescence Technologies for the Investigation of Chemical Libraries. *Mol. Bio Syst.* **2006**, *2*, 380-387.